Optimal Power Allocation for a Full-Duplex Multicarrier Decode-Forward Relay System with or without Direct Link

Lei Chen, Weixiao Meng, Yingbo Hua

PII: S0165-1684(17)30024-5
DOI: 10.1016/j.sigpro.2017.01.014
Reference: SIGPRO 6373

To appear in: *Signal Processing*

Received date: 5 July 2016
Revised date: 24 December 2016
Accepted date: 16 January 2017

Please cite this article as: Lei Chen, Weixiao Meng, Yingbo Hua, Optimal Power Allocation for a Full-Duplex Multicarrier Decode-Forward Relay System with or without Direct Link, *Signal Processing* (2017), doi: 10.1016/j.sigpro.2017.01.014

Highlights

- This paper addresses power allocation problems for a dual-hop full-duplex multicarrier decode-forward relay system with or without a direct link from the source to the destination. The full-duplex relay has a residual self-interference proportional to its transmitted power. We consider two schemes of decode-forward at the relay: carrier-wise decode-forward (CDF) and group-wise decode-forward (GDF).
- For the CDF scheme, we consider problems of optimal power allocation subject to system-wise total power constraint, node-wise individual power constraint and system-wise rate constraint, respectively. All these problems are shown to be equivalent to convex problems, and fast algorithms for finding the exact solutions are developed.
- For the GDF scheme, we focus on the case of node-wise individual power constraint. This problem is non-convex for which we develop fast algorithms for finding locally optimal solutions.
- Using the algorithms developed in this paper, we are able to show that the system capacity with optimal power allocation based on either CDF or GDF is higher than that of the half-duplex relay (HDR) system at power levels where HDR outperforms the direct transmission via the direct link. Furthermore, the system capacity based on GDF is consistently higher than that of HDR for all power levels while both have the same degree of freedom.
- This paper also shows new insights of algorithmic development, which should be useful for other related problems.

ELSEVIER

Available online at www.sciencedirect.com

ScienceDirect

Signal Processing

Signal Processing 00 (2017) 1–42

Optimal Power Allocation for a Full-Duplex Multicarrier Decode-Forward Relay System with or without Direct Link

Lei Chen[a,b], Weixiao Meng[a], Yingbo Hua[b,*]

[a] *Communications Research Center, Harbin Institute of Technology, Harbin, China.*
[b] *Department of Electrical and Computer Engineering, University of California, Riverside, CA 92521, USA*

Abstract

This paper addresses power allocation problems for a dual-hop full-duplex multicarrier decode-forward relay system with or without a direct link from the source to the destination. The full-duplex relay has a residual self-interference proportional to its transmitted power. We consider two schemes of decode-forward at the relay: carrier-wise decode-forward (CDF) and group-wise decode-forward (GDF). For the CDF scheme, we consider problems of optimal power allocation subject to system-wise total power constraint, node-wise individual power constraint and system-wise rate constraint, respectively. All these problems are shown to be equivalent to convex problems, and fast algorithms for finding the exact solutions are developed. For the GDF scheme, we focus on the case of node-wise individual power constraint. This problem is non-convex for which we develop fast algorithms for finding locally optimal solutions. Using the algorithms developed in this paper, we are able to show that the system capacity with optimal power allocation based on either CDF or GDF is higher than that of the half-duplex relay (HDR) system at power levels where HDR outperforms the direct transmission via the direct link. Furthermore, the system capacity based on GDF is consistently higher than that of HDR for all power levels while both have the same degree of freedom. This paper also shows new insights of algorithmic development, which should be useful for other related problems.

Keywords: Full-duplex, decode-forward, multicarrier relay, optimal power allocation.

1. Introduction

It is widely known that wireless relays are useful for fast and efficient establishment of wireless service, and extending the reach of the Internet into areas with insufficient or no cellular wireless coverage. Wireless relays are particularly useful for enhancement of quality-of-service for users at the edge of a cellular network, and for direct communications between vehicles and other types of nodes in mobile ad hoc networks. All of these are because relays

*Corresponding author
Email addresses: leichen@hit.edu.cn (Lei Chen), wxmeng@hit.edu.cn (Weixiao Meng), yhua@ee.ucr.edu (Yingbo Hua)

can be used to substantially reduce the power loss of radio wave propagation between sources and destinations. There are many articles on the subject of wireless relays, and it remains an active research area [1].

As the world sees an ever increasing level of big data mobile applications, the capacity of wireless links must increase. Additional radio spectrum (such as millimeter wave bands) will likely be made available for commercial applications by Government Regulation Agencies. But no matter how much new radio spectrum will be allocated, such a physical resource is always limited and should be utilized as efficiently as possible. One method for efficient utilization of radio spectrum is known as full-duplex radio which is able to transmit and receive at the same time and same frequency. In order to realize full-duplex radio, many research groups from both industry and academia have been trying to develop the best possible ways for radio self-interference cancellation and/or isolation, such as [2, 3] and [4–8]. Motivated by the importance of relay, broad bandwidth and full-duplex radio, this paper studies a full-duplex multicarrier relay network and in particular focuses on optimal power allocation to maximize the performance of such a relay network.

Relay networks can be categorized by many possible combinations of such features as half-duplex versus full-duplex, MIMO versus non-MIMO, multicarrier versus single-carrier, regenerative versus non-regenerative, and presence versus absence of direct-link. The total number of possible categories just based on the above five features is $2^5 = 32$. Within each category, there could be many subcategories depending on other features such as presence versus absence of residual self-interference at full-duplex radio, use versus no-use of successive interference cancellation for receiving at the relay and/or destination, use versus no-use of dirty paper coding for transmitting at the source and/or relay, and full knowledge versus partial knowledge of the channel state information of the source-relay, source-destination and/or relay-destination links. Further categorizations may include the numbers of sources, relays and/or destinations. Clearly, there are numerous possible setups of relay networks. While many of these have been addressed in the literature, still much more are yet to be explored. In the following, we mention a few of the prior works that are relatively relevant to this work.

Many papers on multicarrier (i.e., OFDM based) relay networks such as [9, 10] and [11–22] assume that the relays operate in half-duplex mode rather than full-duplex mode.

And most of these works address non-regenerative (e.g., amplify-forward) half-duplex relays because the problems of regenerative (e.g., decode-forward) half-duplex relays are generally easy to solve and hence of no further intellectual challenge.

A group of recent papers such as [23, 24] and [25–33] address full-duplex relays. But none of them addresses multicarrier full-duplex decode-forward relay with direct link even though it is well known that a decode-forward relay generally yields a higher capacity than an amplify-forward relay [9]. Another group of recent papers [34–36] study the problems of multicarrier full-duplex decode-forward relays. But their focuses and assumptions still substantially differ from ours in this paper. In particular, unlike [36], we will not assume zero self-interference of full-duplex radio. It is known that all practical full-duplex radios have some level of residual self-interference that increases as the transmitted power from the radio increases.

In this paper, we consider a two-hop full-duplex multicarrier decode-forward relay system[1] as illustrated in Fig. 1, where the residual self-interference of the full-duplex relay and the transmission via the direct link are treated as sources of additional (additive) noise at the relay and the destination respectively. We assume the knowledge of channel amplitudes but not channel phases. Channel phases are known to be much harder to obtain than channel amplitudes. We rule out any coding schemes that heavily rely on full channel state information, which include successive interference cancellation for receiving at relay and/or destination and dirty paper coding for transmitting at source and/or relay. We will consider two decode-forward schemes at the relay: one is carrier-wise decode-forward (CDF) and the other is group-wise decode-forward (GDF). Under the CDF scheme, the relay performs decode-forward on each subcarrier separately. Under the GDF scheme, the relay performs decode-forward on the entire group of subcarriers jointly. These two schemes were also introduced in [37] under different names. But they were not treated with optimal power allocation.

The main contribution in this paper is a novel development of fast algorithms based on the CDF and GDF schemes to compute the optimal power allocations among all subcarriers at the source and the relay to maximize performance of the relay network. By using these algorithms, we will show via simulation that the system capacity based on either CDF or

[1]We use "relay system" and "relay network" interchangeably.

GDF is higher than that of a corresponding half-duplex relay (HDF) system at power levels where the HDF system outperforms the direct transmission via the direct link. We will also show that the GDF full-duplex relay system consistently outperforms the HDF system at all power levels while both have the same degree of freedom. The GDF scheme with optimal power allocation optimally benefits from both full-duplex and (frequency division) half-duplex. The algorithmic insights shown in this paper should also be useful for many other related problems. We like to note that the direct link and the self-interference cause a coupling of the optimal power allocation at the source and the optimal power allocation at the relay. It is this coupling that makes the problem much more difficult than otherwise.

The rest of this paper is organized as follows. The system architecture and signal model of the investigated relay system are detailed in Section 2. In this section, we also introduce the capacity expressions of various transmission schemes including the direct transmission via the direct link, the half-duplex relay scheme, the CDF full-duplex relay scheme, and the GDF full-duplex relay scheme. In Section 3, we develop fast algorithms for optimal power allocation based on the CDF full-duplex scheme. We will consider different problem formulations based on (system-wise) total power constraint, (node-wise) individual power constraint and also (system-wise) rate constraint. We will also study the asymptotical performance of the CDF full-duplex relay system. In Section 3.5, we develop a fast algorithm for optimal power allocation based on the GDF full-duplex scheme. The simulation results are discussed in Section 5. We conclude this paper in Section 6.

2. System model

The relay network is illustrated in Figure 1 where each link has N subcarriers. Because the relay is operating in the full-duplex mode, both the source node and the relay node will transmit through the same frequency band simultaneously. In other words, each of the N subcarriers will be occupied at the same time by the source for transmission, by the relay for reception and transmission, and by the destination for reception.

The relay system has four channels[2]: the source to relay channel $\mathbf{h}_{SR}$, the relay to destination channel $\mathbf{h}_{RD}$, the direct link channel $\mathbf{h}_{SD}$ and the residual self-interference[3]

[2] "channels" and "links" are interchangeable

[3] The residual self-interference channel is the net channel of self-interference after the use of self-

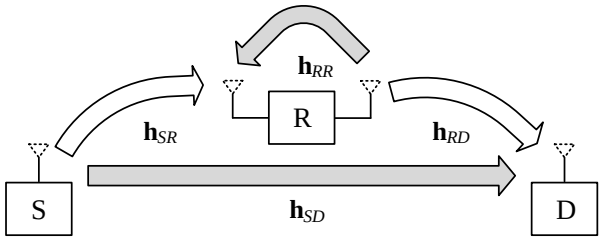

Figure 1. A dual-hop full-duplex DF (decode-forward) multicarrier relay network.

channel $\mathbf{h}_{RR}$. We also use $\mathbf{h}_{SR}$, $\mathbf{h}_{RD}$, $\mathbf{h}_{SD}$ and $\mathbf{h}_{RR}$ to denote the vectors of channel gains. In principle, each of these vectors is a $N \times 1$ complex vector (i.e., in $\mathbb{C}^{N\times 1}$) since each channel has N parallel subcarriers.

Let $\mathbf{x}_S(k)$ and $\mathbf{x}_R(k)$ denote the symbol vectors in $\mathbb{C}^{N\times 1}$ transmitted by the source and the relay respectively at time k. Each of $\mathbf{x}_S(k)$ and $\mathbf{x}_R(k)$ is assumed to have N i.i.d. symbols, which are also statistically stationary in time. Then the vectors of the signals received by the relay and the destination can be expressed as follows[4]:

$$\mathbf{y}_R(k) = \mathbf{h}_{SR} \circ \mathbf{x}_S(k) + \mathbf{h}_{RR} \circ \mathbf{x}_R(k) + \mathbf{n}_R(k), \tag{1}$$

$$\mathbf{y}_D(k) = \mathbf{h}_{RD} \circ \mathbf{x}_R(k) + \mathbf{h}_{SD} \circ \mathbf{x}_S(k) + \mathbf{n}_D(k). \tag{2}$$

Here, the noise vectors $\mathbf{n}_R(k)$ and $\mathbf{n}_D(k)$ are independent of each other and each assumed to be $\mathcal{CN}(0, \mathbf{I})$ (i.e., normalized circular complex Gaussian random vectors). The symbol '$\circ$' indicates the Hadamard product (i.e., element-wise product).

We will use x_n and y_n to denote the powers of the nth elements of $\mathbf{x}_S(k)$ and $\mathbf{x}_R(k)$ at any k, respectively. Also use $A_n = |h_{SRn}|^2$, $B_n = |h_{RRn}|^2$, $C_n = |h_{RDn}|^2$ and $D_n = |h_{SDn}|^2$. Note that h_{SRn} is the nth element of $\mathbf{h}_{SR}$, for example. For optimal power allocation, we will only need these (squared) amplitudes but no phases of the channels.

The (end-to-end) capacity of the relay system depends on further assumptions of transmission and coding schemes. If the power allowed from the source[5] is so high that even

interference suppression and cancellation at radio frequency frontend and/or baseband. For convenience, we will also refer to "residual self-interference channel" as "self-interference channel"

[4]We also assume that both the distortion generated by the limited dynamic range in the transmitter/recevier and the inter-carrier interference leaked from adjacent subcarriers are weak and can be omitted in comparison with the residual self-interference and the direct link interference.

[5]In practice, the power from a source node is not only limited by the power capacity of the source node but also by constraints on its interference to other neighboring networks.

a weak direct link can be used for direct transmission from the source to the destination, then the relay can be simply ignored (i.e., with $y_n = 0, \forall n$). In this case, the capacity in bits/s/Hz of the system is simply

$$\mathcal{R}_{Direct} = \frac{1}{N}\sum_{n=1}^{N}\log_2(1 + D_n x_n) \tag{3}$$

The optimal power allocation to maximize $\mathcal{R}_{Direct}$ follows the classic waterfilling algorithm[6].

If the source power is not high enough for the direct link to deliver a sufficient data rate, a conventional scheme is known as half-duplex relay scheme where in the first time slot the source transmits to the relay and in the second time slot the relay transmits to the destination. In this case, the capacity of the system (with decode-forward relay) is

$$\mathcal{R}_{Half-duplex} = \frac{1}{2}\min(\mathcal{R}_{SR}, \mathcal{R}_{RD}) \tag{4}$$

with $\mathcal{R}_{SR} = \frac{1}{N}\sum_{n=1}^{N}\log_2(1 + A_n x_n)$ and $\mathcal{R}_{RD} = \frac{1}{N}\sum_{n=1}^{N}\log_2(1 + C_n y_n)$. The optimal power allocation to maximize $\mathcal{R}_{Half-dulex}$ is also straightforward by following the waterfilling algorithm.

To improve the spectral efficiency beyond half-duplex, we consider full-duplex relay schemes in this paper. We further assume that there is no cooperative coding between the source and the relay so that the signal from the source via the direct link is treated as an additional noise at the destination[7]. Similarly, the signal from the relay via the self-interference channel is also treated as an additional noise at the receiver of the relay[8].

Consequently, the SINRs (signal to interference and noise ratio) of the received signals on the nth subcarrier at the relay and the destination are respectively:

$$\gamma_{Rn} = \frac{A_n x_n}{1 + B_n y_n}, \tag{5}$$

[6]Subject to $\sum_{n=1}^{N} x_n \le P_S$, $\mathcal{R}_{SD}$ is maximized if $x_n = \max(\lambda - \frac{1}{D_n}, 0)$ with λ satisfying $\sum_{n=1}^{N}\max(\lambda - \frac{1}{D_n}, 0) = P_S$

[7]Such an assumption is also used in [27, 29]

[8]Without the channel phase information of $\mathbf{h}_{RR}$ at the relay, further self-interference cancellation at the relay is not possible. Channel phases change much more rapidly than channel amplitudes and hence much harder to obtain.

$$\gamma_{Dn} = \frac{C_n y_n}{1 + D_n x_n}. \tag{6}$$

At the decode-forward multicarrier relay, the information received on N subcarriers from the source can be re-distributed onto N subcarriers for transmission to the destination in many possible ways. But we will consider two such schemes: carrier-wise decode-forward (CDF) and group-wise decode-forward (GDF). For the CDF scheme, the information received by the relay on each subcarrier is forwarded on the same subcarrier. For the GDF scheme, the information received by the relay on all subcarriers is re-distributed onto all subcarriers optimally for transmission to the destination. The choice of such a scheme depends on application. If the destination node represents a collection of N distributed small nodes and each small node is assigned with one subcarrier (which is a scenario also discussed in [10]), then the carrier-wise scheme is naturally suitable. If the destination node is a single physical node and the relay node is also a single physical node, then the GDF scheme is a natural choice.

With CDF full-duplex relay, the capacity of the relay system (in bits/s/Hz) over M time windows is

$$\begin{aligned} \mathcal{R}_{Full-duplex} &= \frac{M}{M+1}\frac{1}{N}\sum_{n=1}^{N} \min\{\log_2(1+\gamma_{Rn}), \log_2(1+\gamma_{Dn})\} \\ &= \frac{M}{M+1}\frac{1}{N}\sum_{n=1}^{N} \log_2(1+\min\{\gamma_{Rn}, \gamma_{Dn}\}). \end{aligned} \tag{7}$$

For convenience, we will also refer to $\mathcal{R}_{Full-duplex}$ as $\mathcal{R}$.

With RDF full-duplex relay, the capacity of the relay system (in bits/s/Hz) over M time windows[9] is

$$\mathcal{C}_{Full-duplex} = \frac{M}{M+1}\frac{1}{N}\min\left\{\sum_{n=1}^{N}\log_2(1+\gamma_{Rn}), \sum_{n=1}^{N}\log_2(1+\gamma_{Dn})\right\} \tag{8}$$

For convenience, we will also refer to $\mathcal{C}_{Full-duplex}$ as $\mathcal{C}$.

The expressions of both $\mathcal{R}$ and $\mathcal{C}$ are consistent with the previously stated assumption

[9]During each time window, the source transmits a packet to the relay at the same time as the relay transmits a packet to the destination over the same N subcarriers. The packet transmitted by the relay in time window m contains the same information as the packet transmitted by the source in time window $m-1$.

that $\mathbf{x}_S(k)$ and $\mathbf{x}_R(k)$ are stationary random processes[10]. Furthermore, the expression of $\mathcal{C}$ requires cooperative information re-distribution among the subcarriers at the relay so that the sum of the information received by the relay in time window m equals the sum of the information transmitted by the relay in time window $m+1$. Note that even though the relay is full-duplex, the information received by the decode-forward relay during one time window cannot be transmitted by the relay in the same time window. The time window indexed by each $m \in \{1, \cdots, M\}$ needs to be large enough for the capacity $\mathcal{C}$ or $\mathcal{R}$ to be achievable[11]. We will also consider a large M so that $\frac{M}{M+1} \approx 1$.

Obviously, $\mathcal{R}$ is no larger than $\mathcal{C}$. But this property does not necessarily suggest that $\mathcal{C}$ is more useful than $\mathcal{R}$, which was explained previously. In terms of degree of freedom, it is easy to verify that under some weak or typical conditions, $\frac{\mathcal{R}_{Direct}}{\log_2 P} \to 1$, $\frac{\mathcal{R}_{Half-duplex}}{\log_2 P} \to \frac{1}{2}$, and $\frac{\mathcal{C}_{Full-duplex}}{\log_2 P} \to \frac{1}{2}$ as $P = \sum_{n=1}^{N} x_n \to \infty$ and/or $P = \sum_{n=1}^{N} y_n \to \infty$. But as shown later, we typically have $\frac{\mathcal{R}_{Full-duplex}}{\log_2 P} \to 0$. While these degrees of freedom indicate useful trends as the power increases, fast algorithms for optimal power allocation under power constraints are also important in both theory and practice.

Optimal power allocation based on either $\mathcal{R}$ or $\mathcal{C}$ is a challenge not addressed elsewhere (to our best knowledge) but addressed in depth in this paper. In the next section, we will consider $\mathcal{R}$ for optimal power allocation. In section 4, we will consider optimal power allocation based on $\mathcal{C}$. In all cases, we assume that the channel amplitudes (not phases) of the relay system are available to a central scheduler that computes the optimal power allocations to be implemented at the source and the relay.

3. Power Allocation for CDF Full-Duplex Relay

In this section, we first consider the following problem:

$$\begin{aligned} \max_{\mathbf{x},\mathbf{y}} \quad & \mathcal{R} \\ \text{s.t.} \quad & \textit{Power constraints}. \end{aligned} \tag{9}$$

[10]The index k may denote a time both within each time window and across different time windows. A time window also corresponds to the transmission of a data packet.

[11]Approximately achievable in practice

where $\mathbf{x} = [x_1, \cdots, x_N]^T$ (power allocation at the source) and $\mathbf{y} = [y_1, \cdots, y_N]^T$ (power allocation at the relay). The computation of this problem requires a central processor which needs all the channel amplitude information of the relay system. We will investigate two types of power constraints: total (sum) power constraint of the source and the relay, and individual power constraint at each of the source and the relay.

Subject to either of the above two types of power constraints, the following holds:

Lemma 1. *Let (x_n^*, y_n^*) denotes the optimal power allocation for the nth subcarrier. Then,*

$$\gamma_{Rn}(x_n^*, y_n^*) = \gamma_{Dn}(x_n^*, y_n^*). \tag{10}$$

Proof. See Appendix A. The same property was also shown in [27] and [34].

□

3.1. Total power constraint

If we just set an upper bound P_{Total} on the sum power of the source and the relay, we have the following total power constrained problem:

$$\begin{aligned} \max_{\mathbf{x},\mathbf{y}} \quad & \frac{1}{N}\sum_{n=1}^{N} \log_2(1 + \min\{\gamma_{Rn}, \gamma_{Dn}\}) \\ \text{s.t.} \quad & \sum_{n=1}^{N}(x_n + y_n) \le P_{Total}, \\ & x_n \ge 0, y_n \ge 0, \forall n \in \mathsf{N}, \end{aligned} \tag{11}$$

where $\mathsf{N} \doteq \{1, 2, ..., N\}$.

Let $p_n \doteq x_n + y_n$. Then, by *Lemma* 1, we know that for any given p_n, we can obtain x_n and y_n by solving:

$$\begin{cases} \gamma_{Rn} = \gamma_{Dn}, \\ x_n + y_n = p_n, \\ x_n \ge 0, y_n \ge 0. \end{cases} \tag{12}$$

When $A_nD_n - B_nC_n \neq 0$, the solution of the above conditions is

$$\begin{cases} x_n = h_n(p_n) \doteq \dfrac{-(A_n + C_n + 2B_nC_np_n) + \Delta_{3,n}}{2(A_nD_n - B_nC_n)} \\ y_n = l_n(p_n) \doteq \dfrac{(A_n + C_n + 2A_nD_np_n) - \Delta_{3,n}}{2(A_nD_n - B_nC_n)} \end{cases} \tag{13}$$

where

$$\Delta_{3,n} = \sqrt{(A_n + C_n)^2 + 4A_nC_np_n(B_n + D_n + B_nD_np_n)}. \tag{14}$$

When $A_nD_n - B_nC_n = 0$, the solution is

$$\begin{cases} x_n = h_n(p_n) \doteq \dfrac{C_np_n + B_nC_np_n^2}{A_n + C_n + 2B_nC_np_n} \\ y_n = l_n(p_n) \doteq \dfrac{A_np_n + B_nC_np_n^2}{A_n + C_n + 2B_nC_np_n} \end{cases}. \tag{15}$$

In terms of $\mathbf{p} = [p_1, \cdots, p_N]$, the problem (11) reduces to

$$\begin{aligned} \min_{\mathbf{p}} \quad & J_{\mathbf{p}} \\ \text{s.t.} \quad & \sum_{n=1}^{N} p_n = P_{Total}, \\ & p_n \geq 0, \forall n \in \mathsf{N}. \end{aligned} \tag{16}$$

where $J_{\mathbf{p}} = -\frac{1}{N}\sum_{n=1}^{N} \log_2(1 + \frac{A_nh_n(p_n)}{1+B_nl_n(p_n)})$. The equality $\sum_{n=1}^{N} p_n = P_{Total}$ is chosen because $J_{\mathbf{p}}$ is a decreasing function of p_n, $\forall n$. See the last paragraph in Appendix B.

The Karush-Kuhn-Tucker (KKT) conditions of the above problem are

$$\begin{cases} -M_n(p_n) - \lambda_n + \upsilon = 0, \\ \lambda_n p_n = 0, p_n \geq 0, \lambda_n \geq 0, \forall n \in \mathsf{N}, \\ \sum_{n=1}^{N} p_n - P_{Total} = 0 \end{cases} \tag{17}$$

where

$$M_n(p_n) = -\frac{\partial J_{\mathbf{p}}}{\partial p_n} = \frac{\log_2 e}{N} \cdot \frac{A_nh_n'(p_n) - \frac{A_nB_nh_n(p_n)l_n'(p_n)}{1+B_nl_n(p_n)}}{1 + B_nl_n(p_n) + A_nh_n(p_n)}. \tag{18}$$

As shown in Appendix B, $M_n(p_n)$ is a decreasing function of p_n (which suggests that $J_{\mathbf{p}}$

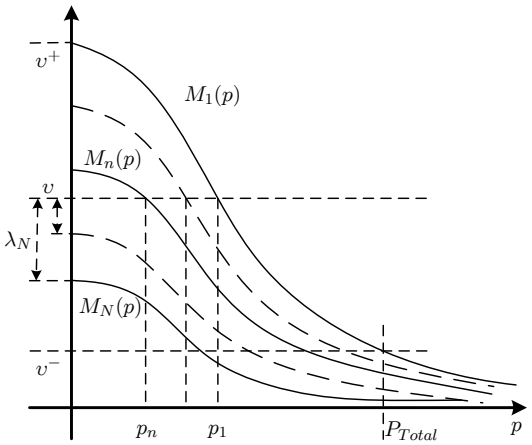

Figure 2. Illustration of the idea behind Algorithm 1.

is convex), utilizing this monotonic property, the KKT conditions in (17) can be solved by Algorithm 1. For the solved p_n, $\forall n$, the x_n and y_n, $\forall n$ can be obtained by substituting p_n, $\forall n$ into (13). The idea behind this algorithm is also illustrated in Fig. 2. In this algorithm, there are two layers of bisection searches. The outer layer searches for the solution of υ. And for each given value of υ, there is an inner layer of N parallel bisection searches for p_n, $\forall n$ (i.e., solving $M_n(p_n) = \upsilon$, $\forall n$). The reason of setting the upper bound $\upsilon^+ = \frac{\log_2 e}{N} \max\{\frac{A_n C_n}{A_n + C_n}, \forall n\}$ is $M_n(0) = \frac{\log_2 e}{N} \frac{A_n C_n}{A_n + C_n}$.

3.2. Individual power constraint

Assuming the total power P_S at the source and the total power P_R at the relay, the individual power constrained problem is:

$$\begin{aligned} \max_{\mathbf{x},\mathbf{y}} \quad & \frac{1}{N} \sum_{n=1}^{N} \log_2(1 + \min\{\gamma_{Rn}, \gamma_{Dn}\}) \\ \text{s.t.} \quad & \sum_{n=1}^{N} x_n \le P_S, \quad \sum_{n=1}^{N} y_n \le P_R, \\ & x_n \ge 0, y_n \ge 0, \forall n \in \mathsf{N}. \end{aligned} \tag{19}$$

Applying *Lemma* 1, we can use $\gamma_{Rn} = \gamma_{Dn}$, and this property implies that the optimal x_n and the optimal y_n are one to one related to each other as shown next .

For any given x_n, solving $\gamma_{Rn} = \gamma_{Dn}$ yields

$$y_n = f_n(x_n) = \frac{-C_n + \Delta_{1,n}}{2B_n C_n}, \tag{20}$$

Algorithm 1 A Two-Layer Bisection Algorithm to Solve (17)

Input:

$A_n, B_n, C_n, D_n, \forall n \in \mathsf{N}$;
Total power constraint P_{Total};
Accuracy threshold ε.

Output:

Initialized upper bound $\upsilon^+ = \frac{\log_2 e}{N} \max\{\frac{A_n C_n}{A_n + C_n}, \forall n\}$;
Initialized lower bound $\upsilon^- = \max\{M_1(P_{Total}), ..., M_N(P_{Total})\}$;
Temporary variable $\mu = 0$;
$p_1 = p_2 =, ..., = p_N = 0$.

while $(|P_{Total} - \mu| > \varepsilon)$ **do**
  $\upsilon = \frac{\upsilon^- + \upsilon^+}{2}$;
  for n=1:N **do**
    if $\upsilon \geq \frac{\log_2 e}{N} \frac{A_n C_n}{A_n + C_n}$ **then**
      $p_n = 0$;
    else
      Solve $M_n(p_n) = \upsilon$;
    end if
  end for
  $\mu = \sum_{n=1}^{N} p_n$;
  if $\mu > P_{Total}$ **then**
    $\upsilon^- = \upsilon$;
  else
    $\upsilon^+ = \upsilon$;
  end if
end while
return $p_1, p_2, ..., p_N$.

where $\Delta_{1,n} = \sqrt{C_n^2 + 4A_n B_n C_n x_n + 4A_n B_n C_n D_n x_n^2}$. Additionally, we have that

$$f_n'(x_n) = \frac{A_n + 2A_n D_n x_n}{\Delta_{1,n}}, \tag{21}$$

$$f_n''(x_n) = \frac{2A_n C_n (D_n C_n - A_n B_n)}{\Delta_{1,n}^3}. \tag{22}$$

We will write

$$\gamma_{Rn,x}(x_n) \doteq \frac{A_n x_n}{1 + B_n f_n(x_n)} = \frac{C_n f_n(x_n)}{1 + D_n x_n} \doteq \gamma_{Dn,x}(x_n). \tag{23}$$

Similarly, for any given y_n, solving $\gamma_{Rn} = \gamma_{Dn}$ yields

$$x_n = g_n(y_n) = \frac{-A_n + \Delta_{2,n}}{2D_n A_n}, \tag{24}$$

where $\Delta_{2,n} = \sqrt{A_n^2 + 4A_nC_nD_ny_n + 4A_nB_nC_nD_ny_n^2}$. We also have that

$$g_n'(y_n) = \frac{C_n + 2C_nB_ny_n}{\Delta_{2,n}}, \tag{25}$$

$$g_n''(y_n) = \frac{2A_nC_n(A_nB_n - C_nD_n)}{\Delta_{2,n}^3}. \tag{26}$$

And we can write

$$\gamma_{Rn,y}(y_n) \doteq \frac{A_ng_n(y_n)}{1 + B_ny_n} = \frac{C_ny_n}{1 + D_ng_n(y_n)} \doteq \gamma_{Dn,y}(y_n). \tag{27}$$

We have shown that the optimal x_n and the optimal y_n are one to one related to each other. Now let

$$\Phi_1 = \{n | C_nD_n - A_nB_n \geq 0, n \in \mathsf{N}\}, \tag{28}$$

and

$$\Phi_2 = \{n | C_nD_n - A_nB_n < 0, n \in \mathsf{N}\}, \tag{29}$$

which are two complementary subsets of N. Also define

$$\mathcal{J}_1 = -\frac{1}{N}\sum_{n_1 \in \Phi_1} \log_2(1 + \frac{A_{n_1}x_{n_1}}{1 + B_{n_1}f_{n_1}(x_{n_1})}), \tag{30}$$

and

$$\mathcal{J}_2 = -\frac{1}{N}\sum_{n_2 \in \Phi_2} \log_2(1 + \frac{C_{n_2}y_{n_2}}{1 + D_{n_2}g_{n_2}(y_{n_2})}). \tag{31}$$

It can be verified that

$$\frac{\partial^2 \mathcal{J}_1}{\partial x_{n_1}^2} \geq 0, \forall n_1 \in \Phi_1, \tag{32}$$

and

$$\frac{\partial^2 \mathcal{J}_2}{\partial y_{n_2}^2} \geq 0, \forall n_2 \in \Phi_2, \tag{33}$$

which means that function $\mathcal{J}_1$ and $\mathcal{J}_2$ are convex functions. See the detailed proof in Appendix C.

With the above preparation, the problem (19) can be transformed into:

$$\begin{aligned} \min_{\mathbf{x}_{\Phi_1},\mathbf{y}_{\Phi_2}} \quad & \mathcal{J}_1+\mathcal{J}_2 \\ \text{s.t.} \quad & \sum_{n_1\in\Phi_1} x_{n_1}+\sum_{n_2\in\Phi_2} g_{n_2}(y_{n_2})\le P_S, \\ & \sum_{n_1\in\Phi_1} f_{n_1}(x_{n_1})+\sum_{n_2\in\Phi_2} y_{n_2}\le P_R \\ & x_{n_1}\ge 0,\forall n_1\in\Phi_1, y_{n_2}\ge 0,\forall n_2\in\Phi_2. \end{aligned} \tag{34}$$

The above problem is a convex problem, i.e., the objective function and the constraints are convex with respect to $\mathbf{x}_{\Phi_1}=\{x_{n_1}\ge 0,\forall n_1\in\Phi_1\}$ and $\mathbf{y}_{\Phi_2}=\{y_{n_2}\ge 0,\forall n_2\in\Phi_2\}$. The Lagrangian function of this problem is:

$$\begin{aligned} L(\mathbf{x}_{\Phi_1},\mathbf{y}_{\Phi_2},\lambda,\upsilon,\boldsymbol{\mu}_1,\boldsymbol{\mu}_2) =& \mathcal{J}_1+\mathcal{J}_2-\boldsymbol{\mu}_1^T\mathbf{x}_{\Phi_1}-\boldsymbol{\mu}_2^T\mathbf{y}_{\Phi_2} \\ & +\lambda\left(\sum_{n_1\in\Phi_1} x_{n_1}+\sum_{n_2\in\Phi_2} g_{n_2}(y_{n_2})-P_S\right) \\ & +\upsilon\left(\sum_{n_1\in\Phi_1} f_{n_1}(x_{n_1})+\sum_{n_2\in\Phi_2} y_{n_2}-P_R\right). \end{aligned} \tag{35}$$

Then, the KKT conditions of the problem (34) are:

$$\begin{cases} \dfrac{\partial L}{\partial x_{n_1}}=-F_{n_1}(x_{n_1})-\mu_{1,n_1}+\lambda+\upsilon f'_{n_1}(x_{n_1})=0, \\ \dfrac{\partial L}{\partial y_{n_2}}=-G_{n_2}(y_{n_2})-\mu_{2,n_2}+\lambda g'_{n_2}(y_{n_2})+\upsilon=0, \\ \lambda\ge 0,\sum\limits_{n_1\in\Phi_1} x_{n_1}+\sum\limits_{n_2\in\Phi_2} g_{n_2}(y_{n_2})\le P_S,\lambda\left(\sum\limits_{n_1\in\Phi_1} x_{n_1}+\sum\limits_{n_2\in\Phi_2} g_{n_2}(y_{n_2})-P_S\right)=0, \\ \upsilon\ge 0,\sum\limits_{n_1\in\Phi_1} f_{n_1}(x_{n_1})+\sum\limits_{n_2\in\Phi_2} y_{n_2}\le P_R,\upsilon\left(\sum\limits_{n_1\in\Phi_1} f_{n_1}(x_{n_1})+\sum\limits_{n_2\in\Phi_2} y_{n_2}-P_R\right)=0, \\ \mu_{1,n_1}\ge 0,x_{n_1}\ge 0,\mu_{1,n_1}x_{n_1}=0,\forall n_1\in\Phi_1, \\ \mu_{2,n_2}\ge 0,y_{n_2}\ge 0,\mu_{2,n_2}y_{n_2}=0,\forall n_2\in\Phi_2, \end{cases} \tag{36}$$

where

$$F_n(x_n) = -\frac{\partial \mathcal{J}_1}{\partial x_n} = \frac{\log_2 e}{N} \cdot \frac{A_n - \frac{A_n B_n x_n f_n'(x_n)}{1+B_n f_n(x_n)}}{1 + B_n f_n(x_n) + A_n x_n}. \tag{37}$$

$$G_n(y_n) = -\frac{\partial \mathcal{J}_2}{\partial y_n} = \frac{\log_2 e}{N} \cdot \frac{C_n - \frac{C_n D_n y_n g_n'(y_n)}{1+D_n g_n(y_n)}}{1 + D_n g_n(y_n) + C_n y_n}. \tag{38}$$

In Appendix C, we prove that the function $F_n(x_n)$ is decreasing with respect to $x_n \in [0, +\infty\}$, and $G_n(x_n)$ is decreasing with respect to $y_n \in [0, +\infty\}$. While, function $f_n'(x_n)$ is increasing with respect to $x_n \in [0, +\infty\}$, and $g_n'(x_n)$ is increasing with respect to $y_n \in [0, +\infty\}$. So, when λ is fixed, υ is a decreasing function with regard to x_n and y_n. When υ is fixed, λ is a decreasing function with regard to x_n and y_n. So, we can utilize a two-dimension bisection search to search for the optimal λ and υ to solve the KKT conditions in (36). The proposed two-dimensional bisection search is summarized as Algorithm 2 along with Algorithms (2.a) and (2.b).

Algorithm 2 Two-Dimensional Bisection Search to Solve (36)

Input:

$A_n, B_n, C_n, D_n, \forall n \in \mathsf{N}$;
Source power constraint P_S, relay power constraint P_R;
Accuracy threshold ϵ.

Output:

1: $\Phi_1 = \{n | C_n D_n - A_n B_n \geq 0, n \in \mathsf{N}\}$, $\Phi_2 = \{n | C_n D_n - A_n B_n < 0, n \in \mathsf{N}\}$;
2: Set $\upsilon = 0$, bisection search of λ, $\mathbf{x}$ and $\mathbf{y}$ to meet $\sum_{n_1 \in \Phi_1} x_{n_1} + \sum_{n_2 \in \Phi_2} g_{n_2}(y_{n_2}) = P_S$, the detailed procedures are presented in Sub-Algorithm (2.a).
3: **if** $\sum_1^N y_n < P_R$ **then**
4: **return** $\mathbf{x}$, $\mathbf{y}$;
5: **end if**
6: Set $\lambda = 0$, bisection search of υ, $\mathbf{x}$ and $\mathbf{y}$ to meet $\sum_{n_1 \in \Phi_1} f_{n_1}(x_{n_1}) + \sum_{n_2 \in \Phi_2} y_{n_2} = P_R$, the detailed procedures are presented in Sub-Algorithm (2.b).
7: **if** $\sum_1^N x_n < P_S$ **then**
8: **return** $\mathbf{x}$, $\mathbf{y}$;
9: **end if**
10: **while** (1) **do**
11: Bisection search of λ, $\mathbf{x}$ and $\mathbf{y}$ to meet $\sum_{n_1 \in \Phi_1} x_{n_1} + \sum_{n_2 \in \Phi_2} g_{n_2}(y_{n_2}) = P_S$ for given υ, the detailed procedures are same as Sub-Algorithm (2.a);
12: Bisection search of υ, $\mathbf{x}$ and $\mathbf{y}$ to meet $\sum_{n_1 \in \Phi_1} f_{n_1}(x_{n_1}) + \sum_{n_2 \in \Phi_2} y_{n_2} = P_R$ for given λ, the detailed procedures are same as Sub-Algorithm (2.b);
13: **if** $|P_S - \sum_1^N x_n| \leq \epsilon$ **then**
14: **break**;
15: **end if**
16: **end while**
17: **return** $\mathbf{x}$, $\mathbf{y}$;

Sub-Algorithm (2.a) bisection search of λ, $\mathbf{x}$ and $\mathbf{y}$ to meet $\sum_{n_1\in\Phi_1} x_{n_1} + \sum_{n_2\in\Phi_2} g_{n_2}(y_{n_2}) = P_S$

$\boldsymbol{\lambda}_{MAX} = zeros(N,1)$, $\boldsymbol{\lambda}_{MIN} = zeros(N,1)$;
for $n_1 \in \Phi_1$ **do**
  $\lambda_{MAX,n_1} = F_{n_1}(0) - \upsilon f'_{n_1}(0)$, $\lambda_{MIN,n_1} = F_{n_1}(P_S) - \upsilon f'_{n_1}(P_S)$;
end for
for $n_2 \in \Phi_2$ **do**
  $\lambda_{MAX,n_2} = \frac{G_{n_2}(0)-\upsilon}{g'_{n_2}(0)}$, $\lambda_{MIN,n_2} = \frac{G_{n_2}(f_{n_2}(P_S))-\upsilon}{g'_{n_2}(f_{n_2}(P_S))}$;
end for
$\lambda_{max} = \max(\boldsymbol{\lambda}_{MAX})$, $\lambda_{min} = \max(\boldsymbol{\lambda}_{MIN})$;
while $(|P_S - \sum_{n=1}^{N} x_n| > \epsilon)$ **do**
  $\lambda = \frac{\lambda_{max}+\lambda_{min}}{2}$;
  for $n_1 \in \Phi_1$ **do**
    if $\lambda > \lambda_{MAX,n_1}$ **then**
      $x_{n_1} = 0$;
    else
      Obtain x_{n_1} by solving $-F_n(x_{n_1}) + \lambda + \upsilon f'_{n_1}(x_{n_1}) = 0$;
    end if
    $y_{n_1} = f_{n_1}(x_{n_1})$;
  end for
  for $n_2 \in \Phi_2$ **do**
    if $\lambda > \lambda_{MAX,n_2}$ **then**
      $y_{n_2} = 0$;
    else
      Obtain y_{n_2} by solving $-G_{n_2}(y_{n_2}) + \lambda g'_{n_2}(y_{n_2}) + \upsilon = 0$;
    end if
    $x_{n_2} = g_{n_2}(y_{n_2})$;
  end for
  if $\sum_{n=1}^{N} x_n > P_S$ **then**
    $\lambda_{min} = \lambda$;
  else
    $\lambda_{max} = \lambda$;
  end if
end while
return λ, $\mathbf{x}$, $\mathbf{y}$;

3.3. Power allocation without direct link

We have discussed the optimal power allocation algorithms for the scenario where there can be a direct link from the source to the destination. In this subsection, we consider the special case where the source to destination channel is $\mathbf{h}_{SD} = \mathbf{0}$, i.e., $D_n = |h_{SDn}|^2 = 0, \forall n \in \mathsf{N}$.

With the total power constraint, the optimal power allocation algorithm given by Algorithm 1 is not affected.

With the individual power constraint, the optimal power allocation algorithm is also

Sub-Algorithm (2.b) bisection search of υ, $\mathbf{x}$ and $\mathbf{y}$ to meet $\sum_{n_1\in\Phi_1} f_{n_1}(x_{n_1}) + \sum_{n_2\in\Phi_2} y_{n_2} = P_R$

$\boldsymbol{\upsilon}_{MAX} = zeros(N,1)$, $\boldsymbol{\upsilon}_{MIN} = zeros(N,1)$;
for $n_1 \in \Phi_1$ **do**
  $\upsilon_{MAX,n_1} = \frac{F_{n_1}(0)-\lambda}{f'_{n_1}(0)}$, $\upsilon_{MIN,n_1} = \frac{F_{n_1}(g_{n_1}(P_R))-\lambda}{f'_{n_1}(g_{n_1}(P_R))}$;
end for
for $n_2 \in \Phi_2$ **do**
  $\upsilon_{MAX,n_2} = G_{n_2}(0) - \lambda g'_{n_2}(0)$, $\upsilon_{MIN,n_2} = G_{n_2}(P_R) - \lambda g'_{n_2}(P_R)$;
end for
$\upsilon_{max} = \max(\boldsymbol{\upsilon}_{MAX})$, $\upsilon_{min} = \max(\boldsymbol{\upsilon}_{MIN})$;
while $(|P_R - \sum_{n=1}^{N} y_n| > \epsilon)$ **do**
  $\upsilon = \frac{\upsilon_{max}+\upsilon_{min}}{2}$;
  for $n_1 \in \Phi_1$ **do**
    if $\upsilon > \upsilon_{MAX,n_1}$ **then**
      $x_{n_1} = 0$;
    else
      Obtain x_{n_1} by solving $-F_n(x_{n_1}) + \lambda + \upsilon f'_{n_1}(x_{n_1}) = 0$;
    end if
    $y_{n_1} = f_{n_1}(x_{n_1})$;
  end for
  for $n_2 \in \Phi_2$ **do**
    if $\upsilon > \upsilon_{MAX,n_2}$ **then**
      $y_{n_2} = 0$;
    else
      Obtain y_{n_2} by solving $-G_{n_2}(y_{n_2}) + \lambda g'_{n_2}(y_{n_2}) + \upsilon = 0$;
    end if
    $x_{n_2} = g_{n_2}(y_{n_2})$;
  end for
  if $\sum_{n=1}^{N} y_n > P_R$ **then**
    $\upsilon_{min} = \upsilon$;
  else
    $\upsilon_{max} = \upsilon$;
  end if
end while
return υ, $\mathbf{x}$, $\mathbf{y}$;

given by Algorithm 2 along with Algorithms (2.a) and (2.b) but with much simplification. To show this, we start with the following (without the direct link):

$$x_n = g_n(y_n) = \frac{C_n y_n + B_n C_n y_n^2}{A_n}, \tag{39}$$

$$g'_n(y_n) = \frac{C_n + 2B_n C_n y_n}{A_n}, \tag{40}$$

Then, the problem (19) reduces to

$$\begin{aligned} \min_{\mathbf{y}} \quad & -\frac{1}{N}\sum_{n=1}^{N}\log_2\left(1+C_n y_n\right) \\ \text{s.t.} \quad & \sum_{n=1}^{N} g_n(y_n) \le P_S, \sum_{n=1}^{N} y_n \le P_R \\ & y_n \ge 0, \forall n \in \{1,2,...,N\}. \end{aligned} \tag{41}$$

The Lagrangian function of this problem is

$$L(\mathbf{y},\lambda,\upsilon,\boldsymbol{\mu}) = -\frac{1}{N}\sum_{n=1}^{N}\log_2\left(1+C_n y_n\right) - \boldsymbol{\mu}^T\mathbf{y} + \lambda\left(\sum_{n=1}^{N} g_n(y_n) - P_S\right) + \upsilon\left(\sum_{n=1}^{N} y_n - P_R\right). \tag{42}$$

Then, the KKT conditions of the problem (41) are:

$$\begin{cases} \dfrac{\partial L}{\partial y_n} = -\dfrac{\log_2 e}{N}\dfrac{C_n}{1+C_n y_n} - \mu_n + \lambda g_n'(y_n) + \upsilon = 0, \\ \lambda \ge 0, \sum_{n=1}^{N} g_n(y_n) \le P_S, \lambda\left(\sum_{n=1}^{N} g_n(y_n) - P_S\right) = 0, \\ \upsilon \ge 0, \sum_{n=1}^{N} y_n \le P_R, \upsilon\left(\sum_{n=1}^{N} y_n - P_R\right) = 0, \\ \mu_n \ge 0, y_n \ge 0, \mu_n y_n = 0, \forall n \in \{1,2,...,N\}. \end{cases} \tag{43}$$

Clearly, the above KKT conditions can be solved by Algorithm 2 along with Algorithms (2.a) and (2.b) and by setting $\Phi_1 = \emptyset$ and $\Phi_2 = \mathsf{N}$. Also, for given λ and υ, the equation $-\frac{\log_2 e}{N}\frac{C_n}{1+C_n y_n} + \lambda g_n'(y_n) + \upsilon = 0$, $\forall n$, is equivalent to a quadratic polynomial equation and has a closed form solution, which is not the case if there is a direct link where $D_n \neq 0$.

3.4. Asymptotic Performance

Proposition 1. *If $B_n > 0$ and $D_n > 0$, $\forall n$, then as the optimal power in each subcarrier becomes large, the end-to-end capacity $\mathcal{R}$ approaches its upper bound $\tilde{\mathcal{R}}$, where*

$$\tilde{\mathcal{R}} \doteq \frac{1}{N}\sum_{n=1}^{N}\log_2\left(1+\sqrt{\frac{A_n C_n}{B_n D_n}}\right). \tag{44}$$

Proof. Given $B_n > 0$ and $D_n > 0$, $\forall n$, then as x_n and y_n, $\forall n$, become large , γ_{Rn} and γ_{Dn}

reduce to

$$\gamma_{Rn} = \frac{A_n x_n}{B_n y_n}, \tag{45}$$

$$\gamma_{Dn} = \frac{C_n y_n}{D_n x_n}. \tag{46}$$

Furthermore, by *Lemma* 1, the optimal power allocations x_n^* and y_n^* must be such that $\gamma_{Rn} = \gamma_{Dn}$, which leads to

$$\frac{x_n^*}{y_n^*} = \sqrt{\frac{B_n C_n}{A_n D_n}}. \tag{47}$$

Therefore, one can verify that $\mathcal{R} \to \tilde{\mathcal{R}}$. Since $\mathcal{R}$ is an increasing function of x_n^* and y_n^*, $\tilde{\mathcal{R}}$ is the upper bound of $\mathcal{R}$.

□

It is easy to show that if there is a non-empty subset S_0 such that $B_n D_n = 0$ and $A_n C_n \neq 0$ for $n \in S_0$, i.e., there is one or more subcarrier where either the direct link or the self-interference is absent while other links are present, then $\max \mathcal{R} \to \infty$ as $P_S \to \infty$ and $P_R \to \infty$. For example, if $A_n \neq 0$, $B_n \neq 0$, $C_n \neq 0$ but $D_n = 0$, then we can have $y_n \to \infty$ and $\frac{x_n}{y_n} \to \infty$ such that $\gamma_{R_n} = \frac{A_n x_n}{1+B_n y_n} = \gamma_{D_n} = C_n y_n \to \infty$ as $P_S \to \infty$ and $P_R \to \infty$.

3.5. Power allocation under rate constraint

In the previous subsections, we have investigated the optimal power allocation under either total power constraint or individual power constraint. In this subsection, we consider how to minimize the total transmitting power under a target end-to-end data rate. This problem can be formulated as

$$\begin{aligned} \min_{\mathbf{x},\mathbf{y}} \quad & \sum_{n=1}^{N} (x_n + y_n) \\ \text{s.t.} \quad & \frac{1}{N} \sum_{n=1}^{N} \log_2(1 + \min\{\gamma_{Rn}, \gamma_{Dn}\}) \geq \mathcal{R}^*, \\ & x_n \geq 0, y_n \geq 0, \forall n \in \mathsf{N}, \end{aligned} \tag{48}$$

where $\mathcal{R}^*$ is the target data rate (which should satisfy $\mathcal{R}^* < \tilde{\mathcal{R}}$ if $B_n D_n \neq 0$).

Applying *Lemma 1* and the fact that the system capacity is a increasing function of the

total power (see Appendix B), the above optimization problem is equivalent to:

$$\begin{aligned} \min_{\mathbf{p}} \quad & \sum_{n=1}^{N} p_n \\ \text{s.t.} \quad & \frac{1}{N}\sum_{n=1}^{N} \log_2\left(1+\frac{A_n h_n(p_n)}{1+B_n l_n(p_n)}\right) = \mathcal{R}^*, \\ & p_n \geq 0, \forall n \in \mathsf{N}, \end{aligned} \tag{49}$$

where $p_n = x_n + y_n$, $h_n(p_n)$ and $l_n(p_n)$ are presented in (13) and (15). Here, we have transformed an inequality constraint in the previous form into an equality constraint in the current form, and reduced the number of variables.

The KKT conditions of the above problem are:

$$\begin{cases} 1-\lambda_n+\upsilon M_n(p_n)=0, \forall n \in \mathsf{N} \\ \lambda_n p_n = 0, \forall n \in \{1,2,...,N\} \\ \frac{1}{N}\sum_{n=1}^{N} \log_2\left(1+\frac{A_n h_n(p_n)}{1+B_n l_n(p_n)}\right) - \mathcal{R}^* = 0 \\ p_n \geq 0, \lambda_n \geq 0, \forall n \in \{1,2,...,N\} \end{cases} \tag{50}$$

where $M_n(p_n)$ is shown in (18). Since $M_n(p_n)$ is decreasing with p_n, a two-layer bisection search algorithm can be formulated (using an idea similar to that of Algorithm 1) to solve (50). The details of the algorithm are omitted.

4. Power Allocation for GDF Full-Duplex Relay

In the previous sections, we have presented power allocation algorithms based on the carrier-wise decode-forward scheme. We have seen that the system capacity $\mathcal{R}$ is generally saturated as the power at the source and the relay becomes large. In other words, the degree of freedom of $\mathcal{R}$ is generally zero, i.e., $\frac{\mathcal{R}}{\log_2 P} \to 0$ as $P = P_S = P_R \to \infty$.

In this section, we will investigate the power allocation algorithm for the group-wise decode-forward scheme. For this scheme, it is easy to show that the system capacity $\mathcal{C}$ as in (8) is no longer upper bounded as the power increases but rather has a degree of freedom equal to 0.5 if N is even. This degree of freedom is achieved when one half of the subcarriers

are used by the source for transmission and the other half of the subcarriers are used by the relay for transmission. In this case, there is no self-interference at the relay nor interference via the direct link at the destination, and $\frac{\mathcal{C}}{\log_2 P} \to 0.5$ as $P = P_S = P_R \to \infty$. This particular scenario is also equivalent to a half-duplex relay network. Therefore, the system capacity $\mathcal{C}$ inherently benefits from both the full-duplex mode and the half-duplex mode. In the following, we will develop fast algorithms for optimal power allocations to maximize $\mathcal{C}$ subject to power constraints.

Since the source and the relay typically have separated power sources, the individual power constraint is often more meaningful than the total power constraint. Hence, in this section, we will only consider the individual power constraint. The power allocation problem now is:

$$\begin{aligned} \max_{\mathbf{x},\mathbf{y}} \quad & \min\left\{\frac{1}{N}\sum_{n=1}^{N}\log_2\left(1+\frac{A_n x_n}{1+B_n y_n}\right), \frac{1}{N}\sum_{n=1}^{N}\log_2\left(1+\frac{C_n y_n}{1+D_n x_n}\right)\right\} \\ s.t. \quad & \sum_{n=1}^{N} x_n \le P_S, \sum_{n=1}^{N} y_n \le P_R, x_n \ge 0, y_n \ge 0, \forall n \in \mathsf{N} \end{aligned} \tag{51}$$

Lemma 2. *Let* $(\mathbf{x}^*, \mathbf{y}^*)$ *denote the solution to the problem (51), it holds that*

$$\frac{1}{N}\sum_{n=1}^{N}\log_2\left(1+\frac{A_n x_n^*}{1+B_n y_n^*}\right) = \frac{1}{N}\sum_{n=1}^{N}\log_2\left(1+\frac{C_n y_n^*}{1+D_n x_n^*}\right). \tag{52}$$

Proof. The proof is similar to that of *Lemma* 1, and is omitted here.

□

Then, the problem (51) can be transformed into:

$$\begin{aligned} \min_{\mathbf{x},\mathbf{y}} \quad & -\frac{1}{N}\sum_{n=1}^{N}\log_2\left(1+\frac{A_n x_n}{1+B_n y_n}\right) \\ s.t. \quad & \frac{1}{N}\sum_{n=1}^{N}\log_2\left(1+\frac{A_n x_n}{1+B_n y_n}\right) = \frac{1}{N}\sum_{n=1}^{N}\log_2\left(1+\frac{C_n y_n}{1+D_n x_n}\right) \\ & \sum_{n=1}^{N} x_n \le P_S, \sum_{n=1}^{N} y_n \le P_R, x_n \ge 0, y_n \ge 0, \forall n \in \mathsf{N}. \end{aligned} \tag{53}$$

The new optimization problem (53) has the same solution as the original problem (51).

And the non-differentiable objective function in (51) has been transformed into a differentiable one in (53). However, the problem (53) is still a non-convex problem. Here, we propose a two-phase iteration algorithm to find a locally optimal solution. This algorithm iterates between a source phase and a relay phase. In the source phase, we compute the optimal source power allocation with a given relay power allocation; and in the relay phase, we compute the optimal relay power allocation for a given source power allocation. The two-phase iteration algorithm is a special case of *block coordinate descent type methods*, and is guaranteed to be locally convergent [38].

4.1. The source-phase computation

With a given relay power allocation, the problem (53) reduces to:

$$\begin{aligned} \min_{\mathbf{x}} \quad & -\frac{1}{N}\sum_{n=1}^{N}\log_2\left(1+\frac{A_n x_n}{1+B_n y_n}\right) \\ s.t. \quad & \frac{1}{N}\sum_{n=1}^{N}\log_2\left(1+\frac{A_n x_n}{1+B_n y_n}\right)=\frac{1}{N}\sum_{n=1}^{N}\log_2\left(1+\frac{C_n y_n}{1+D_n x_n}\right) \\ & \sum_{n=1}^{N} x_n \le P_S, x_n \ge 0, \forall n \in \mathsf{N}. \end{aligned} \tag{54}$$

This problem is still non-convex. We will now use a *sequential convex programming (SCP) method* [39] to relax this non-convex problem into a convex problem by sequential linearization.

Let

$$H(\mathbf{x}) = \frac{1}{N}\sum_{n=1}^{N}\log_2\left(1+\frac{A_n x_n}{1+B_n y_n}\right) - \frac{1}{N}\sum_{n=1}^{N}\log_2\left(1+\frac{C_n y_n}{1+D_n x_n}\right) \tag{55}$$

By the first order Taylor's series expansion around $\mathbf{x}=\mathbf{x}^{(k)}$, $H(\mathbf{x})$ can be approximated as:

$$\begin{aligned} H_T(\mathbf{x},\mathbf{x}^{(k)}) &= H(\mathbf{x}^{(k)}) + (\nabla H(\mathbf{x}^{(k)}))^T(\mathbf{x}-\mathbf{x}^{(k)}) \\ &= H(\mathbf{x}^{(k)}) + \sum_{n=1}^{N}\phi_n(x_n - x_n^{(k)}), \end{aligned} \tag{56}$$

where

$$\phi_n = \frac{\log_2 e}{N}\left(\frac{A_n}{1+A_n x_n^{(k)}+B_n y_n} - \frac{D_n}{1+D_n x_n^{(k)}+C_n y_n} + \frac{D_n}{1+D_n x_n^{(k)}}\right). \tag{57}$$

We compute the updated estimate $\mathbf{x}^{(k+1)}$ by the following:

$$\begin{aligned}\mathbf{x}^{k+1} = \arg\min_{\mathbf{x}} &\left\{-\frac{1}{N}\sum_{n=1}^{N}\log_2\left(1+\frac{A_n x_n}{1+B_n y_n}\right)\right\}\\ s.t.\quad & H_T(\mathbf{x},\mathbf{x}^{(k)})=0, \sum_{n=1}^{N} x_n \le P_S,\\ & x_n \ge 0, \forall n \in \mathsf{N}.\end{aligned} \tag{58}$$

The Lagrangian function of this problem is:

$$L(\mathbf{x},\lambda,\upsilon,\boldsymbol{\mu}) = -\frac{1}{N}\sum_{n=1}^{N}\log_2\left(1+\frac{A_n x_n}{1+B_n y_n}\right) + \lambda H_T(\mathbf{x},\mathbf{x}^{(k)}) + \upsilon\left(\sum_{n=1}^{N} x_n - P_S\right) - \boldsymbol{\mu}^T\mathbf{x}. \tag{59}$$

The KKT conditions of (58) are:

$$\begin{cases}\dfrac{\partial L}{\partial x_n} = -\dfrac{\log_2 e}{N}\dfrac{A_n}{1+A_n x_n + B_n y_n} + \lambda\phi_n + \upsilon - \mu_n = 0,\\ H_T(\mathbf{x},\mathbf{x}^{(k)}) = 0,\\ \upsilon \ge 0, \sum_{n=1}^{N} x_n - P_S \le 0, \upsilon\left(\sum_{n=1}^{N} x_n - P_S\right) = 0,\\ x_n \ge 0, \mu_n \ge 0, \mu_n x_n = 0, \forall n \in \mathsf{N}.\end{cases} \tag{60}$$

From the first equation of (60), if λ is fixed, υ is a decreasing function of x_n, and if υ is fixed, λ is also a decreasing function of x_n. Hence, the conditions of (60) can be solved by a two-dimensional bisection search, which is summarized as Algorithm 3.

4.2. The relay-phase computation

With a given source power allocation, the problem (53) reduces to

$$\begin{aligned}\min_{\mathbf{y}}\quad & -\frac{1}{N}\sum_{n=1}^{N}\log_2\left(1+\frac{C_n y_n}{1+D_n x_n}\right)\\ s.t.\quad & \frac{1}{N}\sum_{n=1}^{N}\log_2\left(1+\frac{A_n x_n}{1+B_n y_n}\right) = \frac{1}{N}\sum_{n=1}^{N}\log_2\left(1+\frac{C_n y_n}{1+D_n x_n}\right)\\ & \sum_{n=1}^{N} y_n \le P_R, y_n \ge 0, \forall n \in \mathsf{N}.\end{aligned} \tag{61}$$

Algorithm 3 Two-dimensional bisection search to find the solution to (60)

Input:

$A_n, B_n, C_n, D_n, y_n, \forall n \in \mathsf{N}$;
Source power constraint P_S;
Accuracy threshold ε.

Output:

Set $\upsilon = 0$, bisection search of λ and $\mathbf{x}$ to meet $H_T(\mathbf{x}, \mathbf{x}^{(k)}) = 0$;
if $\sum_1^N x_n < P_S$ **then**
  return $\mathbf{x}$;
else
  while (1) **do**
    Bisection search of λ and $\mathbf{x}$ to meet $H_T(\mathbf{x}, \mathbf{x}^{(k)}) = 0$ for given υ;
    Bisection search of υ and $\mathbf{x}$ to meet $\sum_1^N x_n = P_S$ for given λ;
    if $|H_T(\mathbf{x}, \mathbf{x}^{(k)}| < \varepsilon$ **then**
      break;
    end if
  end while
  return $\mathbf{x}$.
end if

This problem is similar to that of (54) and can be solved by a similar algorithm as Algorithm 3. We will omit the details.

4.3. Initialization

The two-phase iteration algorithm is locally convergent. The result of the algorithm may depend on the initialization of $x_n, y_n, \forall n$. There are many possible ways to do the initialization. We have tried two as follows:

Method 1: $x_n \forall n$ is such that $\mathcal{R}_{SR} = \frac{1}{N}\sum_{n=1}^N \log_2(1 + A_n x_n)$ is maximized subject to $\sum_{n=1}^N x_n \le P_S$. And $y_n \forall n$ is such that $\mathcal{R}_{RD} = \frac{1}{N}\sum_{n=1}^N \log_2(1 + C_n y_n)$ is maximized subject to $\sum_{n=1}^N y_n \le P_R$. This method effectively ignores all the interferences at the relay and the destination.

Method 2: $x_n \forall n$ is such that $\mathcal{R}_{SR}$ is maximized subject to $\sum_{n=1}^N x_n \le P_S$ *and* $x_n = 0, \forall n \notin \mathsf{N}_x$. And $y_n \forall n$ is such that $\mathcal{R}_{RD}$ is maximized subject to $\sum_{n=1}^N y_n \le P_R$ *and* $y_n = 0, \forall n \notin \mathsf{N}_y$. Here, $\mathsf{N}_x \bigcup \mathsf{N}_y = \mathsf{N}$, and N_x is half (or approximate half if N is odd) of the set N. In the simulation, we will choose N to be even and $\mathsf{N}_x = \{1, \cdots, \frac{N}{2}\}$.

By simulation, we have found that the optimal results starting from the two methods of initialization are somewhat different. In the higher power region, e.g., the per subcarrier power is $\Delta P > 40$dB, method 2 is better. But in the lower power region, e.g., $\Delta P < 40$dB, method 1 is better. Our explanation is that at higher power the frequency-division

half-duplex is closer to the globally optimal solution, but at lower power the impact of interferences at the relay and the destination is relatively small. We have used method 1 for all simulation examples except Fig. 13. In this figure, we used both methods of initialization and then chose the better result.

5. Simulation and Discussion

All algorithms developed in this paper have been tested in Matlab successfully. For the case of carrier-wise decode-forward, all the problems formulated have been reduced *equivalently* to their convex versions, and hence the globally optimal solutions are achieved by our algorithms. For the case of group-wise decode-forward, locally optimal solutions are obtained by our algorithms. Since our algorithms are designed with a full exploitation of the problem structures, they are much faster than using a general purpose convex optimization package and more suitable for real-time applications where channel gains/attenuations may change rapidly.

For the simulation examples to be shown, we choose the channel parameters based on $\mathbf{h}_{SR} \sim \mathcal{CN}(0, \sigma_{SR}^2\mathbf{I})$, $\mathbf{h}_{RR} \sim \mathcal{CN}(0, \sigma_{RR}^2\mathbf{I})$, $\mathbf{h}_{RD} \sim \mathcal{CN}(0, \sigma_{RD}^2\mathbf{I})$, and $\mathbf{h}_{SD} \sim \mathcal{CN}(0, \sigma_{SD}^2\mathbf{I})$. We let $P_{Total} = N\Delta P$ where ΔP denotes the per-subcarrier power. We set $N = 8$, $\sigma_{SR}^2 = \sigma_{RD}^2 = 0$ dB, $\sigma_{RR}^2 = -10$ dB and $\sigma_{SD}^2 = -20$ dB for all examples unless stated otherwise.

5.1. Carrier-wise decode-forward

Shown in Fig. 3 are the results under individual power constraint with three different values of λ such that $P_S = \lambda P_{Total}$ and $P_R = (1-\lambda)P_{Total}$. We see that for each value of λ, the *optimal allocation* of powers by the optimization algorithm yields much higher capacity than *uniform allocation* of powers. With the direct link, Fig. 3(a) shows that as the power increases the system capacities based on *optimal allocations* all converge to their common upper bound $\tilde{\mathcal{R}}$ while the system capacities based on *uniform allocation* saturate at values much smaller than $\tilde{\mathcal{R}}$. Without the direct link, Fig. 3(b) shows that the system capacities based on *optimal allocation* do not saturate while those based on *uniform allocation* still saturate.

Shown in Fig. 4 are the results under total power constraint. Both the cases with and without the direct link are shown in this figure. Like Fig. 3, Fig. 4 also suggests that the capacity gap between *optimal allocation* and *uniform allocation* is significant.

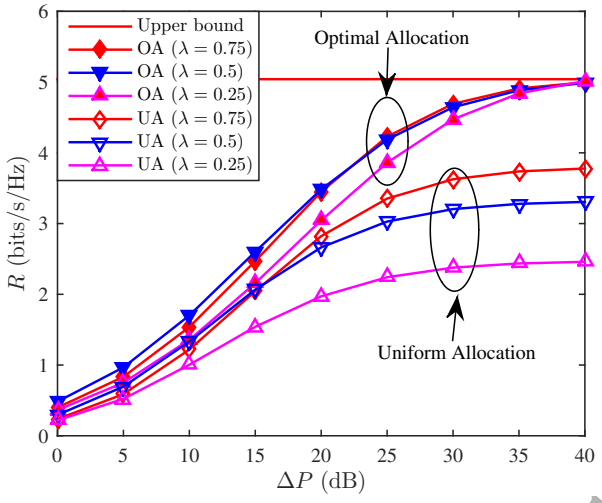

(a) With direct link from source to destination

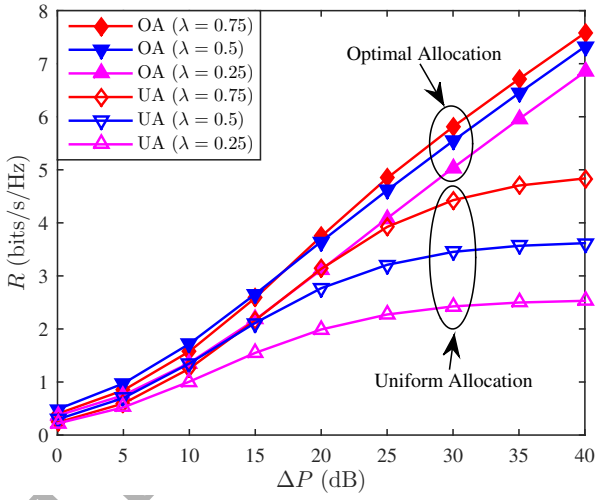

(b) Without direct link from source to destination

Figure 3. Optimal capacity $\mathcal{R}$ vs. per-subcarrier power ΔP under individual power constraint. Averaged over 100 channel realizations. OA denotes optimal allocation, and UA uniform allocation.

Shown in Fig. 5 are two identical curves of *optimal total power versus optimal capacity* achieved either by maximizing the capacity subject to a *total power constraint* $N\Delta P$ or by minimizing the total power subject to a *capacity constraint* R. We see that the two curves are identical as expected. It should be noted that, due to logarithmic scale of P_{Total}, the curve shown in this figure *does not* suggest that the capacity $\mathcal{R}$ increases with P_{Total} faster in the lower power region than in the higher power region. In fact, the contrary is true.

In practice, the number of subcarriers can be large. But there is a good reason not to perform optimal power allocation over the entire set of subcarriers. Shown in Fig. 6 are

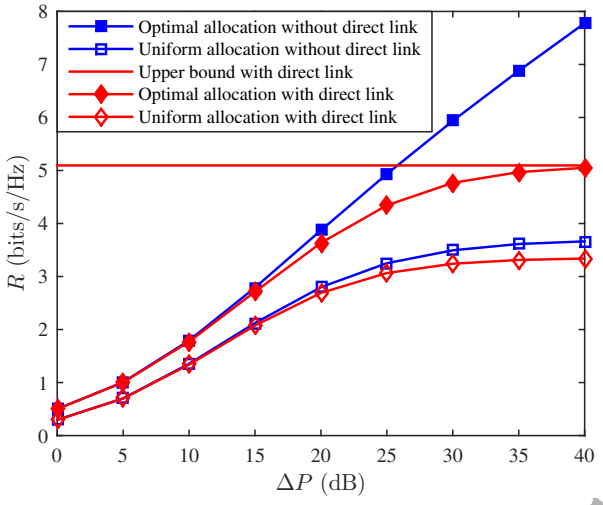

Figure 4. Optimal capacity $\mathcal{R}$ vs. per-subcarrier power ΔP under total power constraint. Averaged over 100 channel realizations.

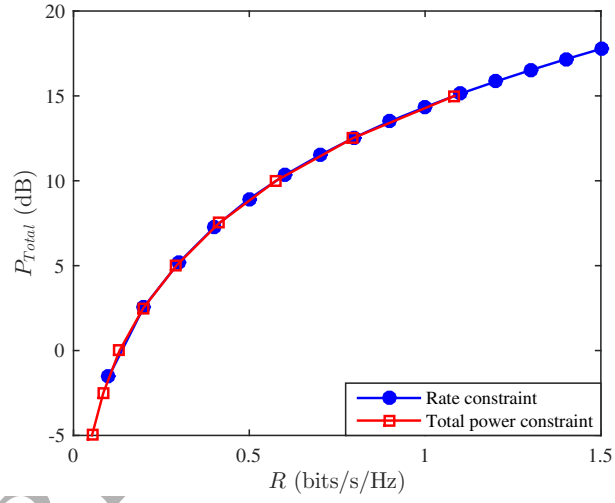

Figure 5. Optimal total power (in dB) vs. optimal capacity under either *total power constraint* or *capacity (rate) constraint*. One channel realization.

curves of the optimal capacity $\mathcal{R}$ versus the number of subcarriers N under individual power constraint. Shown in Fig. 7 are curves of the same but under total power constraint. We see that the impact of N is small when N is large[12]. This suggests a possible way to reduce the complexity as shown next.

[12]If ΔP becomes very large, the impact of N on optimal power allocation diminishes.

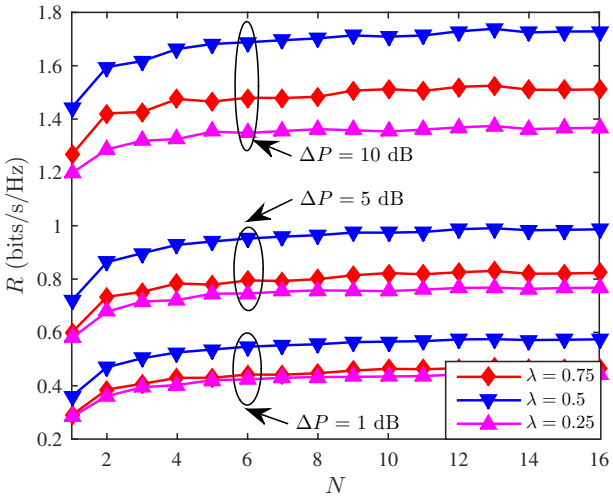

Figure 6. Optimal capacity vs. the number of subcarriers under individual power constraint. Averaged over 1000 channel realizations.

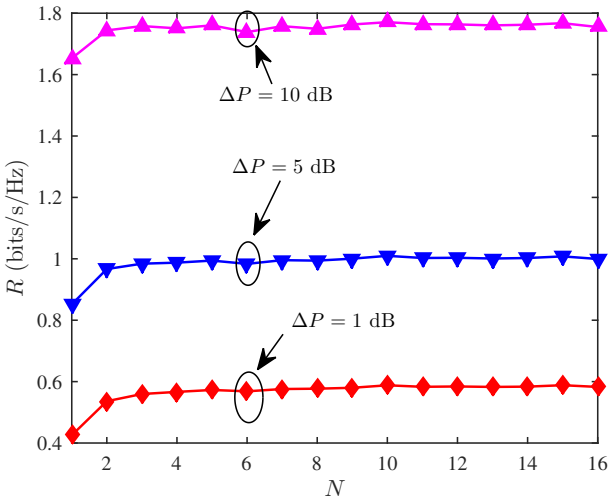

Figure 7. Optimal capacity vs. the number of subcarriers under total power constraint. Averaged over 1000 channel realizations.

The complexity of Algorithm 1 is:

$$\mathcal{O}\left(\log_2(\frac{P}{\varepsilon})\cdot N\cdot\log_2(\frac{P}{\omega})\right). \tag{62}$$

where ε is the precision threshold of the first layer bisection search, and ω is the same of the second layer bisection search (which solves $M_n(p_n)=\upsilon$ for p_n when given *upsilon*). The complexity scales mostly linearly with N. For a large N, we can reduce the complexity with little loss of performance by dividing the N subcarriers into several smaller groups. All these

groups can be handled in parallel with equal shares of total powers, and each group can be handled more efficiently in computation. For better diversity, the subcarriers from different groups may need to interleave with each other.

The performances shown in Fig. 8 and Fig. 9 are examples of the above simplified approach with $N = K\Delta N = 16$, i.e., K groups with each group containing ΔN subcarriers. We see that for $\Delta N = 4$, the simplified approach is very close in performance to the optimal approach. Note that when $\Delta N = 1$, the total power is divided evenly among all N subcarriers. But unlike *uniform allocation* which is also shown in these two figures, the simplified approach optimally adjusts the power in each subcarrier for both the source and the relay. For this reason, the simplified approach even with $\Delta N = 1$ is far better than the uniform distribution of power.

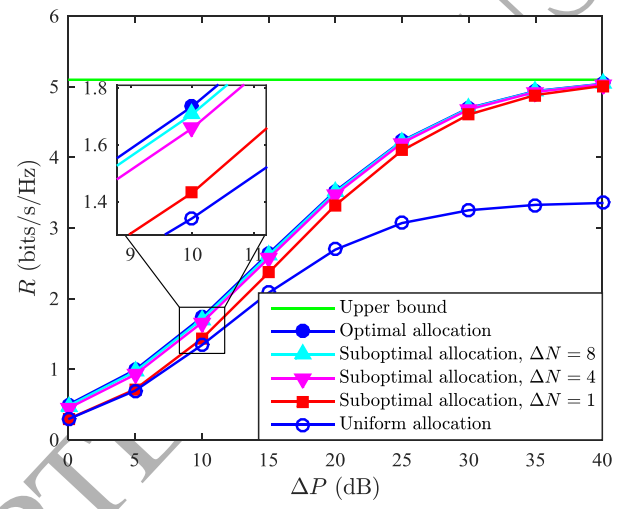

Figure 8. Optimal allocation vs. sub-optimal (simplified) allocation under individual power constraint. $N = K\Delta N = 16$ and $P_S = P_R = 0.5P_{Total} = 0.5N\Delta P$. Averaged over 100 channel realizations.

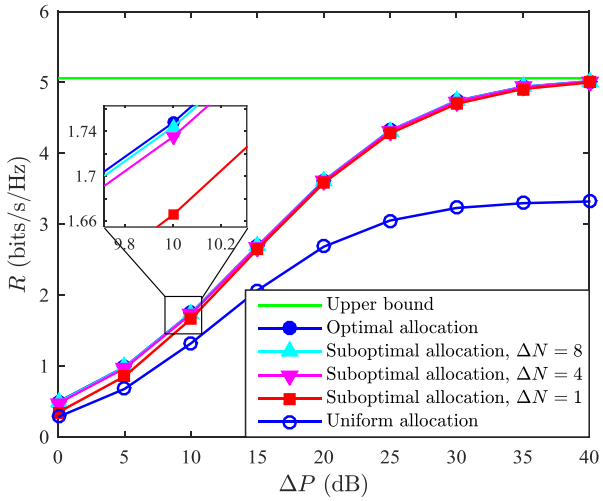

Figure 9. Optimal allocation vs. sub-optimal (simplified) allocation under total power constraint. $N = K\Delta N = 16$ and $P_{Total} = N\Delta P$. Averaged over 100 channel realizations.

5.2. Group-wise decode-forward

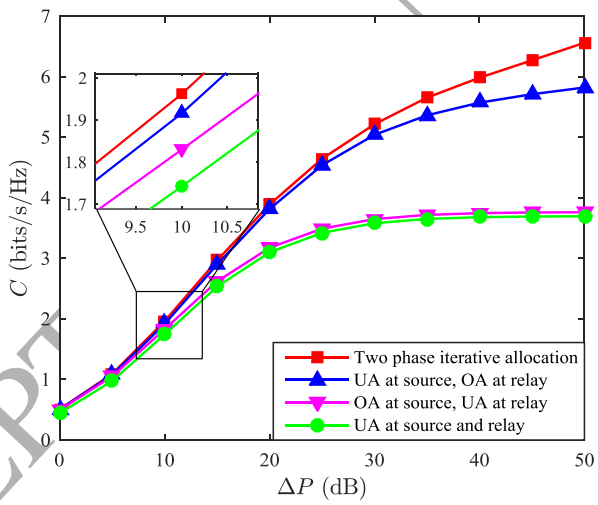

Figure 10. Optimal capacity $\mathcal{C}$ vs. per-subcarrier power ΔP of group-wise decode-forward. Averaged over 100 channel realizations. OA means optimal allocation of power, and UA means uniform allocation of power.

Shown in Fig. 10 are four curves of the optimal capacity $\mathcal{C}$ versus the per-subcarrier power ΔP of the relay system with group-wise decode-forward and individual power constraint. The four curves correspond to the four cases: UA (uniform allocation of power) at both the source and the relay; OA (optimal allocation of power) at the source and UA at the relay; and OA at both the source and the relay via the two-phase iteration. We see that in the low power region the optimization for the relay alone is as good as the optimization for both

the source and the relay. This is because the noise caused by the self-interference at the relay (with $\sigma_{RR}^2 = -10$dB) is stronger than the noise caused by the source via the direct link (with $\sigma_{SD}^2 = -20$dB). But in the high power region, the joint optimization becomes important. This is because the noise caused by the source via the direct link increases as the power from the source increases.

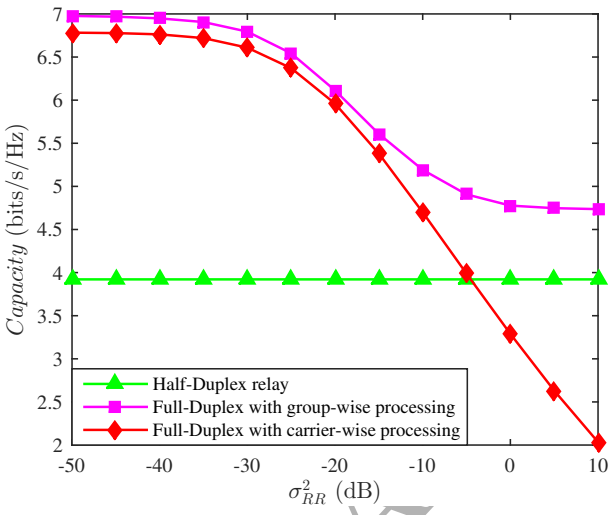

Figure 11. $\mathcal{R}_{Half-duplex}$, $\mathcal{R} = \mathcal{R}_{Full-duplex}$ and $\mathcal{C} = \mathcal{C}_{Full-duplex}$ versus σ_{RR}^2. Averaged over 100 channel realizations. $\Delta P = 30$dB.

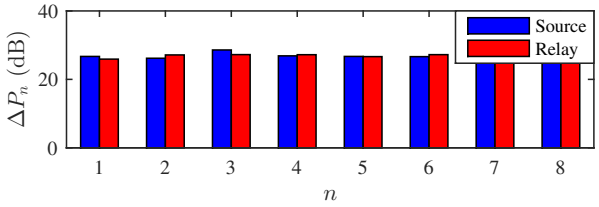

(a) $\sigma_{RR}^2 = -20$ dB

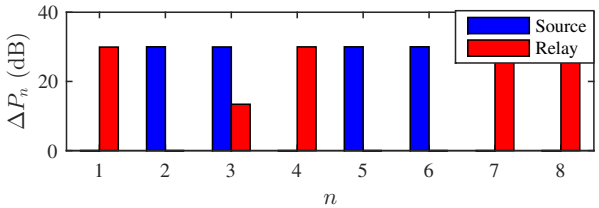

(b) $\sigma_{RR}^2 = 0$ dB

Figure 12. Optimal power allocation results at source and relay for the group-wise protocol when $\Delta P = 30$dB. The horizontal axis n indicates the nth subcarrier.

5.3. Comparison of $\mathcal{R}_{Half-duplex}$, $\mathcal{R}$, $\mathcal{C}$ and more

While keeping $\sigma_{SR}^2 = \sigma_{RD}^2 = 0$ dB and $\sigma_{SD}^2 = -20$ dB, we now let σ_{RR}^2 be a variable. Shown as Fig. 11 is a comparison of the (maximized) capacities of the half-duplex scheme $\mathcal{R}_{Half-duplex}$, the full-duplex scheme with carrier-wise decode-forward $\mathcal{R}$ and the full-duplex scheme with group-wise decode-forward $\mathcal{C}$ as the strength σ_{RR}^2 of the self-interference channel varies. We see that $\mathcal{R}_{Half-duplex}$ stays constant as expected while both $\mathcal{R}$ and $\mathcal{C}$ decrease as σ_{RR}^2 increases. However, $\mathcal{C}$ always stays higher than $\mathcal{R}_{Half-duplex}$ no matter how large σ_{RR}^2 becomes[13]. This is because, with optimal power allocation based on group-wise decode-forward, the relay system automatically transforms into frequency-division half-duplex as σ_{RR}^2 becomes large.

Fig. 12 confirms the transformation. Fig. 12(a) shows the optimal power allocation results when the self-interference is weak ($\sigma_{RR}^2 = -20$dB). In this case, all subcarriers are fully occupied by both the source and the relay for transmission. Fig. 12(b) shows the same but when the self-interference is strong ($\sigma_{RR}^2 = 0$dB). In this case, the source uses one half of the subcarriers for transmission and the relay uses *mostly* the other half for transmission. Yet, the 3rd subcarrier is still utilized by the relay in the full-duplex mode. In other words, the optimized $\mathcal{C}$ benefits from both half-duplex and full-duplex, and hence is always larger than $\mathcal{R}_{Half-duplex}$.

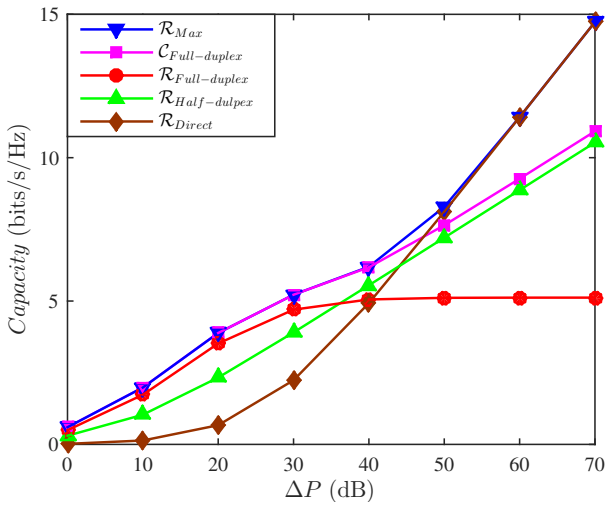

Figure 13. Five optimized capacities versus ΔP. Averaged over 100 channel realizations.

[13]Due to the noise via the direct link, $\mathcal{C} < 2\mathcal{R}_{Half-duplex}$ even if $\sigma_{RR}^2 = 0$.

In Fig. 13, we compare the five optimized capacities (as ΔP varies): the direction transmission from the source to the relay $\mathcal{R}_{direct}$, the half-duplex decode-forward scheme $\mathcal{R}_{Half-duplex}$, the full-duplex carrier-wise decode-forward $\mathcal{R} = \mathcal{R}_{Full-duplex}$, the full-duplex group-wise decode-forward $\mathcal{C} = \mathcal{C}_{Full-duplex}$ and the hybrid scheme $\mathcal{R}_{Max} = \max(\mathcal{R}_{direct}, \mathcal{C})$. We see that, when the power is very high (e.g., $\Delta P > 50$dB), the direction transmission scheme outperforms all other schemes as expected. We also see that, in the high power region, $\mathcal{C}$ and $\mathcal{R}_{Half-duplex}$ move in parallel, which is also expected since both have the degree of freedom equal to $\frac{1}{2}$. In practice, we can hardly afford to have $\Delta P > 50$dB due to limited power resources as well as constrained interference to other neighboring networks. For moderate power levels, e.g., $\Delta P < 30$dB, we see that both $\mathcal{R}$ and $\mathcal{C}$ exceed $\mathcal{R}_{Half-duplex}$ and $\mathcal{R}_{direct}$.

6. Conclusion

In this paper, we have explored the optimal power allocation problems of a dual-hop multi-carrier relay system using a decode-forward full-duplex relay. We allow the presence of the direct link from the source to the destination and a residual level of self-interference at the full-duplex relay. We have considered two schemes of multi-carrier decode-forward: carrier-wise and group-wise. For the carrier-wise scheme, we have transformed the original problems into equivalent convex problems and developed fast algorithms to find the exact optimal solutions. For the group-wise scheme, we have developed a locally convergent fast algorithm. The simulation results based on our algorithms consistently show that both schemes yield higher system capacities than the half-duplex scheme at power levels where the half-duplex scheme outperforms the direct transmission via the direct link.

The algorithms developed require channel amplitude information but not channel phase information. The coding schemes on which the power allocation problems in this paper are formulated have a standard complexity without the need for dirty paper coding at transmitters and/or successive interference cancellation at receivers. The optimal power allocation algorithms based on both $\mathcal{R}_{Full-duplex}$ and $\mathcal{C}_{Full-duplex}$ are important. We believe that the insights shown in this paper can be applied to solve many other related problems.

Appendix A. Proof of Lemma 1

Note that γ_{Rn} increases with x_n and decreases with y_n, while γ_{Dn} decreases with x_n and increases with y_n. Let (x_n^*, y_n^*) denote the optimal power allocation of the nth subcarrier, which maximizes $\min\{\gamma_{R_n}, \gamma_{D_n}\}$. If $\gamma_{Rn}(x_n^*, y_n^*) > \gamma_{Dn}(x_n^*, y_n^*)$, we could increase $\gamma_{Dn}(x_n^*, y_n^*)$ and hence $\min\{\gamma_{R_n}, \gamma_{D_n}\}$ by reducing x_n^*. If $\gamma_{Rn}(x_n^*, y_n^*) < \gamma_{Dn}(x_n^*, y_n^*)$, we could increase $\gamma_{Rn}(x_n^*, y_n^*)$ and hence $\min\{\gamma_{R_n}, \gamma_{D_n}\}$ by reducing y_n^*. Therefore, we must have $\gamma_{Rn}(x_n^*, y_n^*) = \gamma_{Dn}(x_n^*, y_n^*)$.

Appendix B. Proof of the monotone property of $M_n(p_n)$

In this appendix, we will prove that the function $M_n(p_n)$ defined in (18) is decreasing with respect to $p_n \in [0, +\infty\}$. To simply the expression, we ignore the subscript n in the following.

Taking the derivative of $M(p)$, we have

$$M'(p) = \frac{\log_2 e}{N} \frac{\alpha'(p)\beta(p) - \alpha(p)\beta'(p)}{\beta^2(p)}, \tag{B.1}$$

where

$$\begin{aligned} \alpha(p) &= Ah'(p)(1 + Bl(p)) - ABh(p)l'(p), \\ \alpha'(p) &= Ah''(p) + AB(h''(p)l(p) - h(p)l''(p)), \\ \beta(p) &= (1 + Bl(p))^2 + Ah(p)(1 + Bl(p)), \\ \beta'(p) &= (1 + Bl(p))(2Bl'(p) + Ah'(p)) + ABh(p)l'(p). \end{aligned} \tag{B.2}$$

Case 1 where $AD - BC \neq 0$: It follows that

$$\begin{aligned} h'(p) &= \frac{1}{AD - BC}\left[-BC + \frac{AC(B + D) + 2ABCDp}{\Delta_3}\right], \\ h''(p) &= \frac{2AC(AB - CD)}{\Delta_3^3}, \\ l'(p) &= \frac{1}{AD - BC}\left[AD - \frac{AC(B + D) + 2ABCDp}{\Delta_3}\right], \\ l''(p) &= \frac{-2AC(AB - CD)}{\Delta_3^3}, \\ \Delta_3 &= \sqrt{(A + C)^2 + 4ACp(B + D) + 4ABCDp^2}. \end{aligned} \tag{B.3}$$

In this case, there are three subcases as discussed below:

Subcase 1 where $AB < DC$: We see that $h''(p) < 0$. Given $\lim_{p\to+\infty} h'(p) = \frac{\sqrt{BC}}{\sqrt{BC}+\sqrt{AD}} > 0$, so $h'(p) > 0, \forall p \in [0, +\infty)$. We also see that $l''(p) > 0$ and $l'(0) = \frac{A}{A+C} > 0$, and hence $l'(p) > 0, \forall p \in [0, +\infty)$. Since $h(p) > 0$ and $l(p) > 0$, so we have $\alpha'(p) < 0$, $\beta(p) > 0$ and $\beta'(p) > 0$. Moreover, because $\alpha'(p) < 0$ and $\lim_{p\to+\infty} \alpha(p) = \frac{A(\sqrt{BCD}+B\sqrt{A})}{2(\sqrt{BCD}+D\sqrt{A})} > 0$, we have $\alpha(p) > 0$. Therefore, $M'(p) < 0$, i.e., $M(p)$ is decreasing with p.

Subcase 2 where $AB = DC$: We have $h''(p) = l''(p) = 0$, $h'(p) = \frac{B}{B+D}$, $l'(p) = \frac{D}{B+D}$, and $\alpha(p) = \frac{AB}{B+D}$. Since $h(p) > 0$ and $l(p) > 0$, it follows that $\alpha(p) > 0$, $\alpha'(p) = 0$, $\beta(p) > 0$, and $\beta'(p) > 0$. Thus, $M'(p) < 0$.

Subcase 3 where $AB > DC$: By $\gamma_R = \gamma_D$ in the equations (12), $M(p)$ can be written as:

$$M(p) = \frac{\log_2 e}{N} \cdot \frac{Cl'(p)(1 + Dh(p)) - CDl(p)h'(p)}{(1 + Dh(p))^2 + Cl(p)(1 + Dh(p))}. \tag{B.4}$$

Taking the derivative, we have

$$M'(p) = \frac{\log_2 e}{N} \cdot \frac{\hat{\alpha}'(p)\hat{\beta}(p) - \hat{\alpha}(p)\hat{\beta}'(p)}{\hat{\beta}^2(p)}, \tag{B.5}$$

where

$$\begin{aligned}
\hat{\alpha}(p) &= Cl'(p)(1 + Dh(p)) - CDl(p)h'(p),\\
\hat{\alpha}'(p) &= Cl''(p) + CD(l''(p)h(p) - l(p)h''(p)),\\
\hat{\beta}(p) &= (1 + Dh(p))^2 + Cl(p)(1 + Dh(p)),\\
\hat{\beta}'(p) &= (1 + Dh(p))(2Dh'(p) + Cl'(p)) + CDl(p)h'(p).
\end{aligned} \tag{B.6}$$

Because $AB > DC$, $l''(p) < 0$. Since $\lim_{p\to+\infty} l'(p) = \frac{\sqrt{AD}}{\sqrt{BC}+\sqrt{AD}} > 0$, so $l'(p) > 0, \forall p \in [0, +\infty)$. Similarly, we have $h''(p) > 0$ and $h'(0) = \frac{C}{A+C} > 0$. Hence, $h'(p) > 0, \forall p \in [0, +\infty)$. By the fact that $h(p) > 0$, $l(p) > 0$, we have $\hat{\alpha}'(p) < 0$, $\hat{\beta}(p) > 0$, and $\hat{\beta}'(p) > 0$. Moreover, because $\hat{\alpha}'(p) < 0$ and $\lim_{p\to+\infty} \hat{\alpha}(p) = \frac{C(\sqrt{ABD}+D\sqrt{C})}{2(\sqrt{ABD}+B\sqrt{C})} > 0$, we obtain that $\hat{\alpha}(p) > 0$. Therefore, $M'(p) < 0$.

Case 2 where $AD - BC = 0$: We have

$$\begin{aligned} h'(p) &= \frac{C(A+C) + 2BC(A+C)p + 2B^2C^2p^2}{(A+C+2BCp)^2}, \\ h''(p) &= \frac{2BC(A^2-C^2)}{(A+C+2BCp)^3}, \\ l'(p) &= \frac{A(A+C) + 2BC(A+C)p + 2B^2C^2p^2}{(A+C+2BCp)^2}, \\ l''(p) &= \frac{2BC(C^2-A^2)}{(A+C+2BCp)^3}. \end{aligned} \tag{B.7}$$

We also have the following three subcases:

Subcase 1 where $A < C$: Then $h''(p) < 0$. Given $\lim_{p\to+\infty} h'(p) = \frac{1}{2} > 0$, hence $h'(p) > 0$. Because $l''(p) > 0$ and $l'(0) = \frac{A}{A+C} > 0$, we have $l'(p) > 0$. Since $h(p) > 0$ and $l(p) > 0$, we have $\alpha'(p) < 0$, $\beta(p) > 0$, and $\beta'(p) > 0$. Since $\alpha'(p) < 0$ and $\lim_{p\to+\infty} \alpha(p) = \frac{A^2+AC}{4C} > 0$, it holds that $\alpha(p) > 0$. Therefore, $M'(p) < 0$.

Subcase 2 where $A = C$: we have $h''(p) = l''(p) = 0$, $h'(p) = \frac{1}{2}$, $l'(p) = \frac{1}{2}$, and $\alpha(p) = \frac{A}{2}$. Since $h(p) > 0$ and $l(p) > 0$, it follows that $\alpha(p) > 0$, $\alpha'(p) = 0$, $\beta(p) > 0$, and $\beta'(p) > 0$. Therefore $M'(p) < 0$.

Subcase 3 where $A > C$: we can write $M(p)$ as (B.4) and the derivative of $M(p)$ as (B.5). Because $A > C$, we have $l''(p) < 0$. Given $\lim_{p\to+\infty} l'(p) = \frac{1}{2} > 0$, then $l'(p) > 0$. By $h''(p) > 0$ and $h'(0) = \frac{C}{A+C} > 0$, we have $h'(p) > 0$. By $h(p) > 0$ and $l(p) > 0$, we have $\hat{\alpha}'(p) < 0$, $\hat{\beta}(p) > 0$, and $\hat{\beta}'(p) > 0$. Because $\hat{\alpha}'(p) < 0$ and $\lim_{p\to+\infty} \hat{\alpha}(p) = \frac{C^2+AC}{4A} > 0$, we obtain that $\hat{\alpha}(p) > 0$. Therefore, $M'(p) < 0$.

Finally, we prove that $M(p)$ is decreasing with p. Note that, by the fact that $M(p)$ is the derivative of $\frac{1}{N}\log_2(1 + \frac{Ah(p)}{1+Bl(p)})$ and $\lim_{p\to+\infty} M(p) = 0$, it is true that $M(p) > 0$ which means $\frac{1}{N}\log_2(1 + \frac{Ah(p)}{1+Bl(p)})$ is increasing with p, so the the system capacity (or the objective function in (11)) is increasing with P_{Total}.

Appendix C. Proof of convexness of $\mathcal{J}_1$ and $\mathcal{J}_2$

To prove the convexness of $\mathcal{J}_1$ and $\mathcal{J}_2$ shown in (30) and (31), let $F_n(x_n) = -\frac{\partial \mathcal{J}_1}{\partial x_n}$ and $G_n(y_n) = -\frac{\partial \mathcal{J}_2}{\partial y_n}$. We only to prove that $F_n(x_n)$ and $G_n(y_n)$ are both decreasing functions. The proof of each case is similar to the other. So, we will only focus on $F_n(x_n)$.

To simplify the expressions, we will ignore the subscript n in the following derivations.

The derivative of $F(x)$ with respect to x is

$$F'(x) = \frac{\log_2 e}{N} \cdot \frac{\alpha(x)\beta(x) - \phi(x)\psi(x)}{(\varphi^2(x) + Ax\varphi(x))^2}, \tag{C.1}$$

where

$$\begin{aligned}
\alpha(x) &= -ABxf''(x), \\
\beta(x) &= \varphi^2(x) + Ax\varphi(x), \\
\phi(x) &= \frac{A}{2}(1 + \frac{C + 2ABx}{\Delta_1}), \\
\psi(x) &= Bf'(x)(2\varphi(x) + Ax) + A\varphi(x), \\
\varphi(x) &= 1 + Bf(x); \\
f'(x) &= \frac{A + 2ADx}{\Delta_1}, \\
f''(x) &= \frac{2AC(DC - AB)}{\Delta_1^3}, \\
\Delta_1 &= \sqrt{C^2 + 4ABCx + 4ABCDx^2}.
\end{aligned} \tag{C.2}$$

For $DC \geq AB$ and $x \geq 0$, we have

$$\alpha(x) \leq 0, \beta(x) > 0, \phi(x) > 0, \psi(x) > 0, \varphi(x) > 0. \tag{C.3}$$

Then, we obtain $F'(x) < 0$.

Based on equation (23), $F(x)$ can be transformed into another form:

$$F(x) = \frac{\log_2 e}{N} \cdot \frac{Cf'(x)(1 + Dx) - CDf(x)}{(1 + Dx)^2 + Cf(x)(1 + Dx)}, \tag{C.4}$$

Taking its derivative with respect to x, we have

$$F'(x) = \frac{1}{N} \cdot \frac{\hat{\alpha}(x)\hat{\beta}(x) - \hat{\phi}(x)\hat{\psi}(x)}{(\hat{\varphi}^2(x) + Cf(x)\hat{\varphi}(x))^2}, \tag{C.5}$$

where,

$$\begin{aligned}
\hat{\alpha}(x) &= C(1+Dx)f''(x),\\
\hat{\beta}(x) &= \hat{\varphi}^2(x) + Cf(x)\hat{\varphi}(x),\\
\hat{\phi}(x) &= \frac{ABC(2Dx+1)+C(AB-CD)}{2B\Delta_{1n}} + \frac{CD}{2B},\\
\hat{\psi}(x) &= \hat{\varphi}(x)(2D+Cf'(x)) + CDf(x),\\
\hat{\varphi}(x) &= 1+Dx;\\
f'(x) &= \frac{A+2ADx}{\Delta_1},\\
f''(x) &= \frac{2AC(DC-AB)}{\Delta_1^3}.
\end{aligned} \tag{C.6}$$

Now we see that for $DC < AB$ and $x \geq 0$, we have

$$\hat{\alpha}(x) < 0, \hat{\beta}(x) > 0, \hat{\phi}(x) > 0, \hat{\psi}(x) > 0, \hat{\varphi}(x) > 0, \tag{C.7}$$

which again imply that $F'(x) < 0$.

Similarly, we can also prove that $G_n(y_n)$ is decreasing with respect to $y_n \in [0, +\infty\}$.

References

[1] Y. Hua, D. W. Bliss, S. Gazor, Y. Rong, Y. Sung, Theories and methods for advanced wireless relays - Issue I, IEEE Journal on Selected Areas in Communications 30 (8) (2012) 1297–1303. doi:10.1109/JSAC.2012.120901.

[2] Y. Hua, Y. Ma, A. Gholian, Y. Li, A. C. Cirik, P. Liang, Radio self-interference cancellation by transmit beamforming, all-analog cancellation and blind digital tuning, Signal Processing 108 (2015) 322 – 340. doi:10.1016/j.sigpro.2014.09.025.

[3] H. Krishnaswamy, G. Zussman, 1 chip 2x the bandwidth, IEEE Spectrum 53 (7) (2016) 38–54. doi:10.1109/MSPEC.2016.7498157.

[4] J. I. Choi, M. Jain, K. Srinivasan, P. Levis, S. Katti, Achieving single channel, full duplex wireless communication, in: Proceedings of the Sixteenth Annual International Conference on Mobile Computing and Networking, MobiCom '10, ACM, New York, NY, USA, 2010, pp. 1–12. doi:10.1145/1859995.1859997.

[5] M. Duarte, A. Sabharwal, Full-duplex wireless communications using off-the-shelf radios: Feasibility and first results, in: 2010 Conference Record of the Forty Fourth Asilomar Conference on Signals, Systems and Computers, 2010, pp. 1558–1562. doi:10.1109/ACSSC.2010.5757799.

[6] T. Riihonen, S. Werner, R. Wichman, Mitigation of loopback self-interference in full-duplex MIMO

relays, IEEE Transactions on Signal Processing 59 (12) (2011) 5983–5993. doi:10.1109/TSP.2011.2164910.

[7] G. Liu, F. R. Yu, H. Ji, V. C. M. Leung, X. Li, In-band full-duplex relaying: A survey, research issues and challenges, IEEE Communications Surveys Tutorials 17 (2) (2015) 500–524. doi:10.1109/COMST.2015.2394324.

[8] A. Sabharwal, P. Schniter, D. Guo, D. W. Bliss, S. Rangarajan, R. Wichman, In-band full-duplex wireless: Challenges and opportunities, IEEE Journal on Selected Areas in Communications 32 (9) (2014) 1637–1652. doi:10.1109/JSAC.2014.2330193.

[9] W. Zhang, U. Mitra, M. Chiang, Optimization of amplify-and-forward multicarrier two-hop transmission, IEEE Transactions on Communications 59 (5) (2011) 1434–1445. doi:10.1109/TCOMM.2011.022811.100017.

[10] Y. Ma, A. Liu, Y. Hua, A dual-phase power allocation scheme for multicarrier relay system with direct link, IEEE Transactions on Signal Processing 62 (1) (2014) 5–16. doi:10.1109/TSP.2013.2283455.

[11] I. Hammerstrom, A. Wittneben, Power allocation schemes for amplify-and-forward MIMO-OFDM relay links, IEEE Transactions on Wireless Communications 6 (8) (2007) 2798–2802. doi:10.1109/TWC.2007.06071.

[12] W. Dang, M. Tao, H. Mu, J. Huang, Subcarrier-pair based resource allocation for cooperative multi-relay OFDM systems, IEEE Transactions on Wireless Communications 9 (5) (2010) 1640–1649. doi:10.1109/TWC.2010.05.090102.

[13] O. Duval, Z. Hasan, E. Hossain, F. Gagnon, V. K. Bhargava, Subcarrier selection and power allocation for amplify-and-forward relaying over OFDM links, IEEE Transactions on Wireless Communications 9 (4) (2010) 1293–1297. doi:10.1109/TWC.2010.04.090950.

[14] Y. U. Jang, E. R. Jeong, Y. H. Lee, A two-step approach to power allocation for OFDM signals over two-way amplify-and-forward relay, IEEE Transactions on Signal Processing 58 (4) (2010) 2426–2430. doi:10.1109/TSP.2010.2040415.

[15] A. Rao, M. D. Nisar, M. S. Alouini, Robust power allocation for multicarrier amplify-and-forward relaying systems, IEEE Transactions on Vehicular Technology 62 (7) (2013) 3475–3481. doi:10.1109/TVT.2013.2252212.

[16] G. A. S. Sidhu, F. Gao, W. Wang, W. Chen, Resource allocation in relay-aided OFDM cognitive radio networks, IEEE Transactions on Vehicular Technology 62 (8) (2013) 3700–3710. doi:10.1109/TVT.2013.2259511.

[17] W. Wang, R. Wu, Capacity maximization for OFDM two-hop relay system with separate power constraints, IEEE Transactions on Vehicular Technology 58 (9) (2009) 4943–4954. doi:10.1109/TVT.2009.2024674.

[18] X. Zhang, M. Tao, W. Jiao, C. S. Ng, End-to-end outage minimization in OFDM based linear relay networks, IEEE Transactions on Communications 57 (10) (2009) 3034–3044. doi:10.1109/TCOMM.2009.10.080223.

[19] H. Boostanimehr, V. K. Bhargava, Selective subcarrier pairing and power allocation for DF OFDM relay systems with perfect and partial CSI, IEEE Transactions on Wireless Communications 10 (12) (2011) 4057–4067. doi:10.1109/TWC.2011.092911.101200.

[20] C. Jeong, I. M. Kim, Optimal power allocation for secure multicarrier relay systems, IEEE Transactions on Signal Processing 59 (11) (2011) 5428–5442. doi:10.1109/TSP.2011.2162956.

[21] T. Wang, L. Vandendorpe, Sum rate maximized resource allocation in multiple df relays aided OFDM transmission, IEEE Journal on Selected Areas in Communications 29 (8) (2011) 1559–1571. doi:10.1109/JSAC.2011.110906.

[22] M. Shaat, F. Bader, Asymptotically optimal resource allocation in OFDM-based cognitive networks with multiple relays, IEEE Transactions on Wireless Communications 11 (3) (2012) 892–897. doi:10.1109/TWC.2012.011012.110880.

[23] B. P. Day, A. R. Margetts, D. W. Bliss, P. Schniter, Full-duplex MIMO relaying: Achievable rates under limited dynamic range, IEEE Journal on Selected Areas in Communications 30 (8) (2012) 1541–1553. doi:10.1109/JSAC.2012.120921.

[24] A. C. Cirik, Y. Rong, Y. Hua, Achievable rates of full-duplex MIMO radios in fast fading channels with imperfect channel estimation, IEEE Transactions on Signal Processing 62 (15) (2014) 3874–3886. doi:10.1109/TSP.2014.2330806.

[25] M. A. Ahmed, C. C. Tsimenidis, A. F. A. Rawi, Performance analysis of full-duplex-MRC-MIMO with self-interference cancellation using null-space-projection, IEEE Transactions on Signal Processing 64 (12) (2016) 3093–3105. doi:10.1109/TSP.2016.2540611.

[26] E. Antonio-Rodriguez, S. Werner, R. Lopez-Valcarce, T. Riihonen, R. Wichman, Wideband full-duplex MIMO relays with blind adaptive self-interference cancellation, Signal Processing 130 (2017) 74 – 85. doi:10.1016/j.sigpro.2016.06.010.

[27] T. Riihonen, S. Werner, R. Wichman, Hybrid full-duplex/half-duplex relaying with transmit power adaptation, Wireless Communications, IEEE Transactions on 10 (9) (2011) 3074–3085. doi:10.1109/TWC.2011.071411.102266.

[28] L. J. Rodriguez, N. H. Tran, T. Le-Ngoc, Optimal power allocation and capacity of full-duplex AF relaying under residual self-interference, IEEE Wireless Communications Letters 3 (2) (2014) 233–236. doi:10.1109/WCL.2014.020614.130831.

[29] L. Chen, S. Han, W. Meng, C. Li, Optimal power allocation for dual-hop full-duplex decode-and-forward relay, IEEE Communications Letters 19 (3) (2015) 471–474. doi:10.1109/LCOMM.2014.2386336.

[30] H. A. Suraweera, I. Krikidis, G. Zheng, C. Yuen, P. J. Smith, Low-complexity end-to-end performance optimization in MIMO full-duplex relay systems, IEEE Transactions on Wireless Communications 13 (2) (2014) 913–927. doi:10.1109/TWC.2013.122313.130608.

[31] J.-H. Lee, O.-S. Shin, Full-duplex relay based on distributed beamforming in multiuser MIMO systems, Vehicular Technology, IEEE Transactions on 62 (4) (2013) 1855–1860. doi:10.1109/TVT.2012.2232324.

[32] Z. Li, Y. Li, J. Wang, T. Wang, M. Peng, W. Wang, Resource allocation for multiuser two-way full-duplex relay networks, in: 2015 IEEE International Conference on Communications (ICC), 2015, pp. 3299–3304. doi:10.1109/ICC.2015.7248833.

[33] D. W. K. Ng, E. S. Lo, R. Schober, Dynamic resource allocation in MIMO-OFDMA systems with full-duplex and hybrid relaying, IEEE Transactions on Communications 60 (5) (2012) 1291–1304. doi:10.1109/TCOMM.2012.031712.110233.

[34] X. Huang, J. He, Q. Li, Q. Zhang, J. Qin, Optimal power allocation for multicarrier secure communications in full-duplex decode-and-forward relay networks, IEEE Communications Letters 18 (12) (2014) 2169–2172. doi:10.1109/LCOMM.2014.2367527.

[35] G. Liu, H. Ji, F. R. Yu, Y. Li, R. Xie, Energy-efficient resource allocation in full-duplex relaying networks, in: 2014 IEEE International Conference on Communications (ICC), 2014, pp. 2400–2405. doi:10.1109/ICC.2014.6883682.

[36] R. H. Gohary, R. Rashtchi, H. Yanikomeroglu, Optimal design and power allocation for multicarrier decode and forward relays, in: 2015 IEEE International Conference on Acoustics, Speech and Signal Processing (ICASSP), 2015, pp. 3133–3137. doi:10.1109/ICASSP.2015.7178548.

[37] T. Riihonen, R. Wichman, S. Werner, Evaluation of OFDM(A) relaying protocols: Capacity analysis in infrastructure framework, IEEE Transactions on Vehicular Technology 61 (1) (2012) 360–374. doi:10.1109/TVT.2011.2175257.

[38] A. Beck, L. Tetruashvili, On the convergence of block coordinate descent type methods, SIAM Journal on Optimization 23 (4) (2013) 2037–2060. doi:10.1137/120887679.

[39] C. Fleury, Sequential Convex Programming for Structural Optimization Problems, Springer Netherlands, Dordrecht, 1993, pp. 531–553. doi:10.1007/978-94-010-9577-8_25.